arXiv:2007.02153v2 [math.ST] 8 Jul 2020

An Empirical Bayes Approach to Shrinkage Estimation on the Manifold of Symmetric Positive-Definite Matrices*†

Chun-Hao Yang[1], Hani Doss[1] and Baba C. Vemuri[2]
[1]Department of Statistics
[2]Department of Computer Information Science & Engineering
University of Florida

December 7, 2023

Abstract

The James-Stein estimator is an estimator of the multivariate normal mean and dominates the maximum likelihood estimator (MLE) under squared error loss. The original work inspired great interest in developing shrinkage estimators for a variety of problems. Nonetheless, research on shrinkage estimation for manifold-valued data is scarce. In this paper, we propose shrinkage estimators for the parameters of the Log-Normal distribution defined on the manifold of $N \times N$ symmetric positive-definite matrices. For this manifold, we choose the Log-Euclidean metric as its Riemannian metric since it is easy to compute and is widely used in applications. By using the Log-Euclidean distance in the loss function, we derive a shrinkage estimator in an analytic form and show that it is asymptotically optimal within a large class of estimators including the MLE, which is the sample Fréchet mean of the data. We demonstrate the performance of the proposed shrinkage estimator via several simulated data experiments. Furthermore, we apply the shrinkage estimator to perform statistical inference in diffusion magnetic resonance imaging problems.

Keywords: Stein's unbiased risk estimate, Fréchet mean, Tweedie's estimator

*This research was in part funded by the NSF grants IIS-1525431 and IIS-1724174 to Vemuri.
†This manuscript has been submitted to a journal.

1 Introduction

Symmetric positive-definite (SPD) matrices are ubiquitous in applications of science and engineering. In computer vision problems, they are encountered in the form of covariance matrices, and in diffusion magnetic resonance imaging, SPD matrices manifest themselves as diffusion tensors which are used to model the diffusion of water molecules and as Cauchy deformation tensors in morphometry to model the deformations. In such applications, the statistical analysis of data must perform geometry-aware computations, i.e. employ methods that take into account the nonlinear geometry of the data space. In most data analysis applications, it is useful to describe the entire dataset with a few summary statistics. For data residing in Euclidean space, this may simply be the sample mean, and we note that for data residing in non-Euclidean spaces, e.g. Riemannian manifolds, the corresponding statistic is the sample Fréchet mean (FM) (Fréchet 1948). The sample FM also plays an important role in different statistical inference methods, e.g. principal geodesic analysis (Fletcher et al. 2003), clustering algorithms, etc. If M is a metric space with metric d, and $x_1, \ldots, x_n \in M$, the sample FM is defined by $\bar{x} = \arg\min_m \sum_{i=1}^n d^2(x_i, m)$. For Riemannian manifolds, the distance is usually chosen to be the intrinsic distance induced by the Riemannian metric. Then, the above optimization problem can be solved by Riemannian gradient descent algorithms (Groisser 2004, Afsari 2011, Moakher 2005). However, Riemannian gradient descent algorithms are usually computationally expensive, and efficient recursive algorithms for computing the sample FM have been presented in the literature for various Riemannian manifolds by Sturm (2003), Ho et al. (2013), Salehian et al. (2015), Chakraborty & Vemuri (2015), Lim & Pálfia (2014) and Chakraborty & Vemuri (2019).

In $\mathbb{R}^p$ with the Euclidean metric, the sample FM is just the ordinary sample mean. Consider a set of normally distributed random variables $X_1, \ldots, X_n$. The sample mean $\bar{X} = n^{-1} \sum_{i=1}^n X_i$ is the maximum likelihood estimator (MLE) for the mean of the underlying normal distribution and the James-Stein (shrinkage) estimator (James & Stein 1962) was shown to be better (under squared error loss) than the MLE when $p > 2$ and the covariance matrix of the underlying normal distribution is assumed to be known. Inspired by this result, the goal of this paper is to develop shrinkage estimators for data residing in P_N, the space

of $N \times N$ SPD matrices.

For the model $X_i \overset{\text{ind}}{\sim} N(\mu_i, \sigma^2)$ where $p > 2$ and σ^2 is known, the MLE of $\mu = [\mu_1, \ldots, \mu_p]^T$ is $\hat{\mu}^{\text{MLE}} = [X_1, \ldots, X_p]^T$ and it is natural to ask whether the MLE is admissible. Stein (1956) gave a negative answer to this question and provided a class of estimators for μ that dominate the MLE. Subsequently, James & Stein (1962) proposed the estimator

$$\left(1 - \frac{(p-2)\sigma^2}{\|X\|^2}\right) X \tag{1}$$

where $X = [X_1, \ldots, X_p]^T$, which was later referred to as the James-Stein (shrinkage) estimator.

Ever since the work reported in James & Stein (1962), generalizations or variants of this shrinkage estimator have been developed in a variety of settings. A few directions for generalization are as follows. First, instead of estimating the means of many normal distributions, carry out the simultaneous estimation of parameters (e.g. the mean or the scale parameter) of other distributions, e.g. Poisson, Gamma, etc.; see Johnson (1971), Fienberg & Holland (1973), Clevenson & Zidek (1975), Tsui (1981), Tsui & Press (1982), Brandwein & Strawderman (1990) and Brandwein & Strawderman (1991). More recent works include Xie et al. (2012), Xie et al. (2016), Jing et al. (2016) and Kong et al. (2017). Second, since the MLE of the mean of a normal distribution is also the best translation-equivariant estimator but is inadmissible, an interesting question to ask is, when is the best translation-equivariant estimator admissible? This problem was studied extensively in Stein (1959) and Brown (1966).

Besides estimation of the mean of different distributions, estimation of the covariance matrix (or the precision matrix) of a multivariate normal distribution is an important problem in statistics, finance, engineering and many other fields. The usual estimator, namely the sample covariance matrix, performs poorly in high-dimensional problems and many researchers have endeavored to improve covariance estimation by applying the concept of shrinkage in this context (Stein 1975, Haff 1991, Daniels & Kass 2001, Ledoit & Wolf 2003, Daniels & Kass 2001, Ledoit & Wolf 2012, Donoho et al. 2018). Note that there is a vast literature on covariance estimation and we only cited a few references here. For a thorough literature review, we refer the interested reader to Donoho et al. (2018).

In order to understand shrinkage estimation fully, one must understand why the process of shrinkage improves estimation. In this context, Efron and Morris presented a series of works to provide an empirical Bayes interpretation by modifying the original James-Stein estimator to suit different problems (Efron & Morris 1971, 1972*b*,*a*, 1973*b*,*a*). The empirical Bayes approach to designing a shrinkage estimator can be described as follows. First, reformulate the model as a Bayesian model, i.e. place a prior on the parameters. Then, the hyper-parameters of the prior are estimated from the data. Efron & Morris (1973*b*) presented several examples of different shrinkage estimators developed within this empirical Bayes framework. An alternative, non-Bayesian, geometric interpretation to Stein shrinkage estimation was presented by Brown & Zhao (2012).

In all the works cited above, the domain of the data has invariably been a vector space and, as mentioned earlier, many applications naturally encounter data residing in non-Euclidean spaces. Hence, generalizing shrinkage estimation to non-Euclidean spaces is a worthwhile pursuit. In this paper, we focus on shrinkage estimation for the Riemannian manifold P_N. We assume that the observed SPD matrices are drawn from a Log-Normal distribution defined on P_N (Schwartzman 2016) and we are interested in estimating the mean and the covariance matrix of this distribution. We derive shrinkage estimators for the parameters of the Log-Normal distribution using an empirical Bayes framework (Xie et al. 2012), which is described in detail subsequently, and show that the proposed estimator is asymptotically optimal within a class of estimators including the MLE. We describe simulated data experiments which demonstrate that the proposed shrinkage estimator of the mean of the Log-Normal distribution is better (in terms of risk) than the widely-used Riemannian gradient descent-based estimator (Bhattacharya & Patrangenaru 2003, 2005) and the recently-developed inductive/recursive FM estimator presented in Ho et al. (2013). Further, we also apply the shrinkage estimator to find group differences between patients with Parkinson's disease and controls (normal subjects) from their respective brain scans acquired using diffusion magnetic resonance images (dMRIs).

The rest of this paper is organized as follows. In section 2, we present relevant material on the Riemannian geometry of P_N and shrinkage estimation. The main theoretical results are stated in section 3 with the proofs of the theorems relegated to the supplement. In section 4,

we demonstrate how the proposed shrinkage estimators perform via several synthetic data examples and present applications to (real data) diffusion tensor imaging (DTI), a clinically popular version of dMRI. Specifically, we apply the proposed shrinkage estimator to the estimation of the brain atlases (templates) of patients with Parkinson's disease and a control group and identify the regions of the brain where the two groups differ significantly. Finally, in section 5 we discuss our contributions and present some future research directions.

2 Preliminaries

In this section, we first present commonly used notation in Riemannian geometry that will be used throughout the paper. For a detailed exposition on this topic, we refer the reader to the excellent text by Boothby (1986). Then, we briefly review two of the most commonly used Riemannian geometries for P_N and refer the reader to more details in Moakher (2005) and Arsigny et al. (2007). Finally, we review the concept of Stein's unbiased risk estimate, which will form the framework for deriving the shrinkage estimators.

2.1 Definitions and Notations

Let (M, g) be an m-dimensional Riemannian manifold. For $p \in M$, the *tangent space* of M at p is denoted T_pM; this is an m-dimensional vector space. The geodesic connecting two points p and q is denoted by $\gamma_{p,q}$. It has the property that $\gamma_{p,q}(0) = p$ and $\gamma_{p,q}(1) = q$. Alternatively, a geodesic can be specified uniquely by its starting point p and its initial direction $v \in T_pM$; in this case, the geodesic is denoted by γ_v and has the properties that $\gamma_v(0) = p$ and $\gamma_v'(0) = v$. Let $D_p \subset T_pM$ be the set of tangent vectors v such that $\gamma_v(1)$ exists. The Riemannian *Exponential map* $\mathbf{Exp}_p : D_p \to M$ is defined by $\mathbf{Exp}_p(v) = \gamma_v(1)$ for $v \in T_pM$. Since the exponential map is a diffeomorphism (see page 33 in Helgason (2001)), its inverse exists and will be denoted by $\mathbf{Log}_p$. These two maps will be of fundamental importance for the derivation of our shrinkage estimators in the next section. The Riemannian distance induced by the Riemannian metric g is denoted by d_g. Let $x_1, \ldots, x_n \in M$. The FM of

$x_1, \ldots, x_n$ is

$$\bar{x} = \arg\min_{m \in M} \sum_{i=1}^{n} d_g^2(x_i, m).$$

Under mild conditions, the FM exists and is unique; for a detailed discussion of these conditions, see Afsari (2011) and Groisser (2004). In most practical situations, these conditions are satisfied.

2.2 Riemannian Geometry of P_N

The Riemannian geometry of P_N is discussed in detail by Helgason (2001) and Terras (2012). There are two commonly used Riemannian geometries for P_N, the GL-invariant geometry and the Log-Euclidean geometry, and each of them has its own advantages and disadvantages. We will briefly review both of them for the sake of completeness and we will focus on the Log-Euclidean geometry.

The Riemannian manifold P_N can be identified with the quotient space $GL(N)/O(N)$ (Terras 2012), where $GL(N)$ denotes the General Linear group (the group of $N \times N$ non-singular matrices), and $O(N)$ is the orthogonal group (the group of $N \times N$ orthogonal matrices). Hence P_N is a homogeneous space with $GL(N)$ as the group that acts on it and the group action defined for any $X \in P_N$ and $g \in GL(N)$ by $X[g] = gXg^T$. One can now define GL-invariant quantities such as the GL-invariant Riemannian metric based on the group action defined above. We will now begin with the inner product in the tangent space of P_N at a point $X \in P_N$. The GL-invariant Riemannian metric is given by

$$\langle U, V \rangle_X = \mathrm{tr}(X^{-1/2} U X^{-1} V X^{-1/2}) \tag{2}$$

for $X \in P_N$ and $U, V \in T_X P_N$. The tangent space $T_I P_N$ of P_N at the identity matrix I is actually the space of $N \times N$ symmetric matrices, denoted by $\mathsf{Sym}(N)$, which is a vector space of dimension $N(N+1)/2$. Hence P_N is a $N(N+1)/2$-dimensional Riemannian manifold. The GL-invariance of this metric is easy to check. With the GL-invariant metric, the induced geodesic distance between $X, Y \in P_N$ is given by

$$d_{\mathrm{GL}}(X, Y) = \sqrt{\mathrm{tr}((\log(X^{-1}Y))^2)} \tag{3}$$

where log is the matrix logarithm (see Terras (2012)). Since this distance is induced from the GL-invariant metric in (2), it is naturally GL-invariant, i.e. $d_{\mathrm{GL}}(X, Y) = d_{\mathrm{GL}}(gXg^T, gYg^T)$. The exponential and log maps on P_N are given by

$$\begin{aligned} \mathbf{Exp}_X(V) &= X^{1/2} \exp(X^{-1/2} V X^{-1/2}) X^{1/2} \\ \mathbf{Log}_X(Y) &= X^{1/2} \log(X^{-1/2} Y X^{-1/2}) X^{1/2}, \end{aligned} \tag{4}$$

where $X, Y \in P_N$ and $V \in T_X P_N$.

Arsigny et al. (2007) proposed the Log-Euclidean metric on the manifold P_N as an alternative to the GL-invariant metric. The Log-Euclidean metric is a bi-invariant Riemannian metric on the Lie group $(P_N, \odot)$ where $X \odot Y = \exp(\log X + \log Y)$. The intrinsic distance $d_{\mathrm{LE}} : P_N \times P_N \to \mathbb{R}$ induced by the Log-Euclidean metric has a very simple form, namely

$$d_{\mathrm{LE}}(X, Y) = \|\log X - \log Y\|$$

where $\|\cdot\|$ is the Frobenius norm. Consider the map $\mathrm{vec} : \mathsf{Sym}(N) \to \mathbb{R}^{\frac{N(N+1)}{2}}$ defined by

$$\mathrm{vec}(Y) = \left[y_{11}, \ldots, y_{nn}, \sqrt{2}(y_{ij})_{i<j} \right]^T$$

(Schwartzman 2016). This map is actually an isomorphism between $\mathsf{Sym}(N)$ and $\mathbb{R}^{\frac{N(N+1)}{2}}$. To make the notation more concise, for $X \in P_N$, we denote $\widetilde{X} = \mathrm{vec}(\log X) \in \mathbb{R}^{\frac{N(N+1)}{2}}$. From the definition of vec, we see that $d_{\mathrm{LE}}(X, Y) = \|\widetilde{X} - \widetilde{Y}\|$.

Given $X_1, \ldots, X_n \in P_N$, we denote the sample FM with respect to the two intrinsic distances given above by

$$\bar{X}_n^{\mathrm{GL}} = \underset{M \in P_N}{\arg\min}\, n^{-1} \sum_{i=1}^{n} d_{GL}^2(X_i, M) \text{ and} \tag{5}$$

$$\bar{X}_n^{\mathrm{LE}} = \underset{M \in P_N}{\arg\min}\, n^{-1} \sum_{i=1}^{n} d_{LE}^2(X_i, M) = \exp\left(n^{-1} \sum_{i=1}^{n} \log X_i \right). \tag{6}$$

2.3 The Log-Normal Distribution on P_N

In this work, we assume that the observed SPD matrices follow the Log-Normal distribution introduced by Schwartzman (2006), which can be viewed as a generalization of the Log-Normal distribution on $\mathbb{R}^+$ to P_N. The definition of the Log-Normal distribution is stated as follows.

Definition 1 Let X be a P_N-valued random variable. We say X follows a Log-Normal distribution with mean $M \in P_N$ and covariance matrix $\Sigma \in P_{N(N+1)/2}$, or $X \sim \mathrm{LN}(M, \Sigma)$, if $\widetilde{X} \sim N(\widetilde{M}, \Sigma)$.

From the definition, it is easy to see that $E \log X = \log M$ and $E\|\log X - \log M\|^2 = E\|\widetilde{X} - \widetilde{M}\|^2 = \mathrm{tr}(\Sigma)$. Some important results regarding this distribution were obtained in Schwartzman (2016). The following proposition for the MLEs of the parameters from Schwartzman (2016) will be useful subsequently in this work.

Proposition 1 *Let $X_1, \ldots, X_n \overset{iid}{\sim} LN(M, \Sigma)$. Then, the MLEs of M and Σ are $\widehat{M}^{MLE} = \bar{X}_n^{LE}$ and $\widehat{\Sigma}^{MLE} = n^{-1} \sum_{i=1}^n \left(\widetilde{X}_i - \widetilde{\hat{M}^{MLE}}\right)\left(\widetilde{X}_i - \widetilde{\hat{M}^{MLE}}\right)^T$. The MLE of M is the sample FM under the Log-Euclidean metric.*

2.4 Bayesian Formulation of Shrinkage Estimation in $\mathbb{R}^p$

As discussed earlier, the James-Stein estimator originated from the problem of simultaneous estimation of multiple means of (univariate) normal distributions. The derivation relied heavily on the properties of the univariate normal distribution. Later on, Efron & Morris (1973*b*) gave an empirical Bayes interpretation for the James-Stein estimator, which is presented by considering the hierarchical model

$$\begin{aligned} X_i|\theta_i &\overset{\text{ind}}{\sim} N(\theta_i, A), \quad i = 1, \ldots, p, \\ \theta_i &\overset{\text{iid}}{\sim} N(\mu, \lambda), \end{aligned}$$

where A is known and μ and λ are unknown. The posterior mean for θ_i is

$$\hat{\theta}_i^{\lambda,\mu} = \frac{\lambda}{\lambda + A} X_i + \frac{A}{\lambda + A}\mu. \tag{7}$$

The parametric empirical Bayes method for estimating the θ_i's consists of first estimating the prior parameters λ and μ and then substituting them into (7). The prior parameters λ and μ can be estimated by the MLE. For the special case of $\mu = 0$, this method produces an estimator similar to the James-Stein estimator (1). Although this estimator is derived in an (empirical) Bayesian framework, it is of interest to determine whether it has good frequentist properties. For example, if we specify a loss function L and consider the induced

risk function R, one would like to determine whether the estimator has uniformly smallest risk within a reasonable class of estimators. In (7), the optimal choice of λ and μ is

$$\left(\hat{\lambda}^{\text{opt}}, \hat{\mu}^{\text{opt}}\right) = \arg\min_{\lambda,\mu} R\left(\hat{\boldsymbol{\theta}}^{\lambda,\mu}, \boldsymbol{\theta}\right),$$

where $\boldsymbol{\theta} = [\theta_1, \ldots, \theta_p]^T$, $\hat{\boldsymbol{\theta}}^{\lambda,\mu} = [\hat{\theta}_1^{\lambda,\mu}, \ldots, \hat{\theta}_p^{\lambda,\mu}]^T$, and $\hat{\lambda}^{\text{opt}}$ and $\hat{\mu}^{\text{opt}}$ depend on $\boldsymbol{\theta}$, which is unknown. Instead of minimizing the risk function directly, we will minimize Stein's unbiased risk estimate (SURE) (Stein 1981), denoted by $\text{SURE}(\lambda, \mu)$, which satisfies $E_{\boldsymbol{\theta}}\left[\text{SURE}(\lambda, \mu)\right] = R(\hat{\boldsymbol{\theta}}^{\lambda,\mu}, \boldsymbol{\theta})$. Thus, we will use

$$\left(\hat{\lambda}^{\text{SURE}}, \hat{\mu}^{\text{SURE}}\right) = \arg\min_{\lambda,\mu} \text{SURE}(\lambda, \mu).$$

The challenging part of this endeavor is to derive SURE, which depends heavily on the risk function and the underlying distribution of the data. This approach has been used to derive estimators for many models. For example, Xie et al. (2012) derived the (asymptotically) optimal shrinkage estimator for a heteroscedastic hierarchical model, and their result is further generalized in Jing et al. (2016) and Kong et al. (2017).

3 An Empirical Bayes Shrinkage Estimator for Log-Normal Distributions

In this section, we consider the model

$$X_{ij} \overset{\text{ind}}{\sim} \text{LN}(M_i, \Sigma_i), \quad i = 1, \ldots, p,\ j = 1, \ldots, n,$$

and develop shrinkage estimators for the mean $\boldsymbol{M} = [M_1, \ldots, M_p]$ and the covariance matrix $\boldsymbol{\Sigma} = [\Sigma_1, \ldots, \Sigma_p]$. These X_{ij}'s are P_N-valued random matrices. For completeness, we first briefly review the shrinkage estimator proposed by Yang & Vemuri (2019) for $\boldsymbol{M}$ assuming $\Sigma_i = A_i I$, where the A_i's are known positive numbers and I is the identity matrix. The assumption on $\boldsymbol{\Sigma}$ is useful when n is small since for small sample sizes the MLE for $\boldsymbol{\Sigma}$ is very unstable. Next, we present estimators for both $\boldsymbol{M}$ and $\boldsymbol{\Sigma}$. Besides presenting these estimators, we establish asymptotic optimality results for the proposed estimators. To be

more precise, we show that the proposed estimators are asymptotically optimal within a large class of estimators containing the MLE.

Another related interesting problem often encountered in practice involves group testing and estimating the "difference" between the two given groups. Consider the model

$$X_{ij} \overset{\text{ind}}{\sim} \text{LN}(M_i^{(1)}, \Sigma_i^{(1)}), \quad i = 1, \ldots, p,\ j = 1, \ldots, n_x,$$
$$Y_{ij} \overset{\text{ind}}{\sim} \text{LN}(M_i^{(2)}, \Sigma_i^{(2)}), \quad i = 1, \ldots, p,\ j = 1, \ldots, n_y,$$

where the X_{ij}'s and Y_{ij}'s are independent. We want to estimate the differences between $M_i^{(1)}$ and $M_i^{(2)}$ for $i = 1, \ldots, p$ and select the i's for which the differences are large. However, the estimates for the selected values tend to overestimate the corresponding true differences. The bias introduced by the selection process is termed by *selection bias* (Dawid 1994). The selection bias originates from the fact that there are two possible reasons for the selected differences to be large: (i) the true differences are large and (ii) the random errors contained in the estimates are large. Tweedie's formula (Efron 2011), which we discuss and briefly review in section 3.3, deals with precisely this selection bias, in the context of the normal means problem. In this work, we apply an analogue of Tweedie's formula designed for the context of SPD matrices.

3.1 An Estimator of $\boldsymbol{M}$ When $\boldsymbol{\Sigma}$ is Known

For completeness, we briefly review the work of Yang & Vemuri (2019) where the authors presented the estimator for $\boldsymbol{M}$ assuming that $\Sigma_i = A_i I$ where the A_i's are known positive numbers. Under this assumption, they considered the class of estimators given by

$$\widehat{M}_i^{\lambda,\mu} = \exp\left(\frac{n\lambda}{n\lambda + A_i} \log \bar{X}_i^{\text{LE}} + \frac{A_i}{n\lambda + A_i} \log \mu\right), \tag{8}$$

where $\mu \in P_N$ and $\lambda > 0$. Using the Log-Euclidean distance as the loss function, they showed that the SURE for the corresponding risk function is given by

$$\text{SURE}(\lambda, \mu) = \frac{1}{p} \sum_{i=1}^{p} \frac{A_i}{(n\lambda + A_i)^2} \left(A_i \|\log \bar{X}_i^{\text{LE}} - \log \mu\|^2 + \frac{q(n^2\lambda^2 - A_i^2)}{n} \right).$$

Hence, λ and μ can be estimated by

$$\left(\hat{\lambda}^{\text{SURE}}, \hat{\mu}^{\text{SURE}}\right) = \arg\min_{\lambda,\mu} \text{SURE}(\lambda, \mu). \tag{9}$$

Their shrinkage estimator for M_i is given by

$$\widehat{M}_i^{\text{SURE}} = \exp\left(\frac{n\hat{\lambda}^{\text{SURE}}}{n\hat{\lambda}^{\text{SURE}} + A_i} \log \bar{X}_i^{\text{LE}} + \frac{A_i}{n\hat{\lambda}^{\text{SURE}} + A_i} \log \hat{\mu}^{\text{SURE}}\right). \tag{10}$$

They also presented the following two theorems showing the asymptotic optimality of the shrinkage estimator.

Theorem 1 *Assume the following conditions:*

(i) $\limsup_{p\to\infty} p^{-1} \sum_{i=1}^{p} A_i^2 < \infty$,

(ii) $\limsup_{p\to\infty} p^{-1} \sum_{i=1}^{p} A_i \|\log M_i\|^2 < \infty$,

(iii) $\limsup_{p\to\infty} p^{-1} \sum_{i=1}^{p} \|\log M_i\|^{2+\delta} < \infty$ *for some* $\delta > 0$.

Then,

$$\sup_{\lambda>0, \|\log \mu\| < \max_i \|\log \bar{X}_i^{LE}\|} |SURE(\lambda, \mu) - L(\widehat{\boldsymbol{M}}^{\lambda,\mu}, \boldsymbol{M})| \xrightarrow{prob} 0 \quad as\ p \to \infty.$$

Theorem 2 *If assumptions (i), (ii) and (iii) in Theorem 1 hold, then*

$$\lim_{p\to\infty} [R(\widehat{\boldsymbol{M}}^{SURE}, \boldsymbol{M}) - R(\widehat{\boldsymbol{M}}^{\lambda,\mu}, \boldsymbol{M})] \leq 0.$$

3.2 Estimators for $\boldsymbol{M}$ and $\boldsymbol{\Sigma}$

In Yang & Vemuri (2019), the covariance matrices of the underlying distributions were assumed to be known to simplify the derivation. In real applications however, the covariance matrices are rarely known, and in practice they must be estimated. In this paper, we consider the general case of unknown covariance matrices which is more challenging and pertinent in real applications. Let

$$\begin{aligned} X_{ij}|(M_i, \Sigma_i) &\overset{\text{ind}}{\sim} \text{LN}(M_i, \Sigma_i) \\ M_i|\Sigma_i &\overset{\text{ind}}{\sim} \text{LN}(\mu, \lambda^{-1}\Sigma_i) \\ \Sigma_i &\overset{\text{iid}}{\sim} \text{Inv-Wishart}(\Psi, \nu), \end{aligned} \tag{11}$$

for $i = 1, \ldots, p$ and $j = 1, \ldots, n$. The prior for (M_i, Σ_i) is called the Log-Normal-Inverse-Wishart (LNIW) prior, and it is motivated by the normal-inverse-Wishart prior in the Euclidean space setting. The main reason for choosing the LNIW prior over others is the

property of conjugacy which leads to a closed-form expression for our estimators. Let

$$\bar{X}_i^{\mathrm{LE}} = \exp\left(n^{-1}\sum_{j=1}^{n}\log X_{ij}\right) \quad \text{and} \quad S_i = \sum_{j=1}^{n}\big(\widetilde{X}_{ij} - \widetilde{\bar{X}_i^{\mathrm{LE}}}\big)\big(\widetilde{X}_{ij} - \widetilde{\bar{X}_i^{\mathrm{LE}}}\big)^T. \tag{12}$$

Then the posterior distributions of M_i and Σ_i are given by

$$M_i|\big(\{X_{ij}\}_{i,j}, \{\Sigma_i\}_{i=1}^p\big) \sim \mathrm{LN}\Big(\exp\Big(\frac{n\log\bar{X}_i^{\mathrm{LE}} + \lambda\log\mu}{\lambda+n}\Big), (\lambda+n)^{-1}\Sigma_i\Big)$$
$$\Sigma_i|S_i \sim \text{Inv-Wishart}(\Psi + S_i, \nu + n - 1),$$

and the posterior means for M_i and Σ_i are given by

$$\widehat{M}_i = \exp\Big(\frac{n\log\bar{X}_i^{\mathrm{LE}} + \lambda\log\mu}{\lambda+n}\Big) \quad \text{and} \quad \widehat{\Sigma}_i = \frac{\Psi + S_i}{\nu+n-q-2}. \tag{13}$$

Consider the loss function

$$\begin{aligned} L\big((\widehat{\boldsymbol{M}}, \widehat{\boldsymbol{\Sigma}}), (\boldsymbol{M}, \boldsymbol{\Sigma})\big) &= p^{-1}\sum_{i=1}^{p} d_{\mathrm{LE}}^2(\widehat{M}_i, M_i) + p^{-1}\sum_{i=1}^{p}\|\widehat{\Sigma}_i - \Sigma_i\| \\ &= L_1(\widehat{\boldsymbol{M}}, \boldsymbol{M}) + L_2(\widehat{\boldsymbol{\Sigma}}, \boldsymbol{\Sigma}). \end{aligned}$$

Its induced risk function is given by

$$\begin{aligned} R\big((\widehat{\boldsymbol{M}}, \widehat{\boldsymbol{\Sigma}}), (\boldsymbol{M}, \boldsymbol{\Sigma})\big) &= p^{-1}\sum_{i=1}^{p} E d_{\mathrm{LE}}^2(\widehat{M}_i, M_i) + E\|\widehat{\Sigma}_i - \Sigma_i\|^2 \\ &= p^{-1}(\lambda+n)^{-2}\sum_{i=1}^{p}\big[n\mathrm{tr}\Sigma_i + \lambda^2 d_{\mathrm{LE}}^2(\mu, M_i)\big] \\ &\quad + p^{-1}\sum_{i=1}^{p}(\nu+n-q-2)^{-2}\Big[\big(n-1+(\nu-q-1)^2\big)\mathrm{tr}(\Sigma_i^2) \\ &\quad - 2(\nu-q-1)\mathrm{tr}(\Psi\Sigma_i) + (n-1)(\mathrm{tr}\Sigma_i)^2 + \mathrm{tr}(\Psi^2)\Big] \end{aligned}$$

with the detailed derivation given in the supplemental material. The SURE for this risk function is

$$\begin{aligned} \mathrm{SURE}(\lambda, \Psi, \nu, \mu) = p^{-1}\Bigg\{ &\sum_{i=1}^{p}(\lambda+n)^{-2}\Big[\frac{n-\lambda^2/n}{n-1}\,\mathrm{tr}\,S_i + \lambda^2 d_{\mathrm{LE}}^2(\bar{X}_i^{\mathrm{LE}}, \mu)\Big] \\ &+ (\nu+n-q-2)^{-2}\Big[\frac{n-3+(\nu-q-1)^2}{(n+1)(n-2)}\,\mathrm{tr}(S_i^2) \\ &+ \frac{(n-1)^2-(\nu-q-1)^2}{(n-1)(n+1)(n-2)}\big(\mathrm{tr}\,S_i\big)^2 - 2\frac{\nu-q-1}{n-1}\,\mathrm{tr}(\Psi S_i) + \mathrm{tr}(\Psi^2)\Big]\Bigg\} \end{aligned}$$

with the detailed derivation given in the supplemental material.

The hyperparameter vector $(\lambda, \Psi, \nu, \mu)$ is estimated by minimizing $\mathrm{SURE}(\lambda, \Psi, \nu, \mu)$, and the resulting shrinkage estimators of M_i and Σ_i are obtained by plugging in the minimizing vector into (13). Note that this is a non-convex optimization problem and for such problems, the convergence relies heavily on the choice of the initialization. We suggest the following initialization, which is discussed in the supplemental material:

$$\begin{aligned}
\mu_0 &= \exp\left(p^{-1}\sum_{i=1}^{p}\log \bar{X}_i^{\mathrm{LE}}\right)\\
\lambda_0 &= \frac{np^{-1}\sum_{i=1}^{p} d^2_{\mathrm{LE}}(\bar{X}_i^{\mathrm{LE}}, \mu_0)}{\frac{n}{p(n-1)}\sum_{i=1}^{p}\operatorname{tr} S_i - p^{-1}\sum_{i=1}^{p} d^2_{\mathrm{LE}}(\bar{X}_i^{\mathrm{LE}}, \mu_0)}\\
\nu_0 &= \frac{q+1}{\frac{n-q-2}{p^2 q(n-1)}\operatorname{tr}\left[\left(\sum_{i=1}^{p} S_i\right)\left(\sum_{i=1}^{p} S_i^{-1}\right)\right] - 1} + q + 1\\
\Psi_0 &= \frac{\nu_0 - q - 1}{p(n-1)}\sum_{i=1}^{p} S_i.
\end{aligned}$$

In all our experiments, the algorithm converged in less than 20 iterations with the suggested initialization. This concludes the description of our estimators of the unknown means and covariance matrices. Theorem 3 below states that $\mathrm{SURE}(\lambda, \Psi, \nu, \mu)$ approximates the true loss $L\big((\widehat{\boldsymbol{M}}^{\lambda,\mu}, \widehat{\boldsymbol{\Sigma}}^{\Psi,\nu}), (\boldsymbol{M}, \boldsymbol{\Sigma})\big)$ well in the sense that the difference between the two random variables converges to 0 in probability as $p \to \infty$. Additionally, Theorem 4 below shows that the estimators of $\boldsymbol{M}$ and $\boldsymbol{\Sigma}$ obtained by minimizing $\mathrm{SURE}(\lambda, \Psi, \nu, \mu)$ are asymptotically optimal in the class of estimators of the form (13).

Theorem 3 *Assume the following conditions:*

(i) $\limsup_{p\to\infty} p^{-1}\sum_{i=1}^{p}\left(\operatorname{tr}\Sigma_i\right)^4 < \infty$,

(ii) $\limsup_{p\to\infty} p^{-1}\sum_{i=1}^{p}\widetilde{M}_i^T\Sigma_i\widetilde{M}_i < \infty$,

(iii) $\limsup_{p\to\infty} p^{-1}\sum_{i=1}^{p}\|\log M_i\|^{2+\delta} < \infty$ *for some* $\delta > 0$.

Then

$$\sup_{\substack{\lambda>0,\nu>q+1,\|\Psi\|\le\max_{1\le i\le p}\|S_i\|,\\ \|\log\mu\|\le\max_{1\le i\le p}\|\log\bar{X}_i^{LE}\|}}\left|SURE(\lambda,\Psi,\nu,\mu) - L\Big((\widehat{\boldsymbol{M}}^{\lambda,\mu}, \widehat{\boldsymbol{\Sigma}}^{\Psi,\nu}), (\boldsymbol{M}, \boldsymbol{\Sigma})\Big)\right| \xrightarrow{prob} 0 \quad as\ p\to\infty.$$

Theorem 4 *If assumptions (i), (ii), and (iii) in Theorem 3 hold, then*

$$\lim_{p\to\infty}\left[R\Big((\widehat{\boldsymbol{M}}^{SURE},\widehat{\boldsymbol{\Sigma}}^{SURE}),(\boldsymbol{M},\boldsymbol{\Sigma})\Big)-R\Big((\widehat{\boldsymbol{M}}^{\lambda,\mu},\widehat{\boldsymbol{\Sigma}}^{\Psi,\nu}),(\boldsymbol{M},\boldsymbol{\Sigma})\Big)\right]\leq 0.$$

Remark: The proofs of Theorems 1 and 2 in Yang & Vemuri (2019) use arguments similar to those that already exist in the literature, and in that sense they are not very difficult. In contrast, the proofs of our Theorems 3 and 4 above do not proceed along familiar lines. Indeed, they are rather complicated, the difficulty being that bounding the moments of Wishart matrices or the moments of trace of Wishart matrices is nontrivial when the orders of the required moments are higher than two. We present these proofs in the supplementary document.

3.3 Tweedie's Formula for F Statistics

One of the motivations for the development of our approach for estimating $\boldsymbol{M}$ and $\boldsymbol{\Sigma}$ is a problem in neuroimaging involving detection of differences between a patient group and a control group. The problem can be stated as follows. There are n_x patients in a disease group and n_y normal subjects in a control group. We consider a region of the brain image consisting of p voxels. As explained in section 4.2, the local diffusional property of water molecules in the human brain is of clinical importance and it is common to capture this diffusional property at each voxel in the diffusion magnetic resonance image (dMRI) via a zero-mean Gaussian with a 3×3 covariance matrix. Using any of the existing state-of-the-art dMRI analysis techniques, it is possible to estimate, from each patient image, the diffusion tensor M_i corresponding to voxel i, for $i=1,\ldots,p$. Let $M_i^{(1)}$ and $M_i^{(2)}$ denote the diffusion tensors corresponding to voxel i for the disease and control groups respectively. The goal is to identify the indices i for which the difference between $M_i^{(1)}$ and $M_i^{(2)}$ is large. The model we consider is

$$\begin{aligned} X_{ij} &\overset{\text{ind}}{\sim} \text{LN}(M_i^{(1)},\Sigma_i), \quad i=1,\ldots,\ j=1,\ldots,n_x,\\ Y_{ij} &\overset{\text{ind}}{\sim} \text{LN}(M_i^{(2)},\Sigma_i), \quad i=1,\ldots,\ j=1,\ldots,n_y. \end{aligned}$$

In this work, we compute the Hotelling T^2 statistic for each $i=1,\ldots,p$ as a measure of

the difference between $M_i^{(1)}$ and $M_i^{(2)}$. The Hotelling T^2 statistic is given by

$$t_i^2 = \left(\widetilde{\bar{X}_i^{\text{LE}}} - \widetilde{\bar{Y}_i^{\text{LE}}}\right)^T \left[\left(\frac{1}{n_x} + \frac{1}{n_y}\right) S_i\right]^{-1} \left(\widetilde{\bar{X}_i^{\text{LE}}} - \widetilde{\bar{Y}_i^{\text{LE}}}\right) \tag{14}$$

where $\bar{X}_i^{\text{LE}}$ and $\bar{Y}_i^{\text{LE}}$ are the FMs of $\{X_{ij}\}_j$ and $\{Y_{ij}\}_j$ and $S_i = (n_x + n_y - 2)^{-1}\left(S_i^{(1)} + S_i^{(2)}\right)$ is the pooled estimate of Σ_i where $S_i^{(1)}$ and $S_i^{(2)}$ are computed using (12). Since the X_{ij}'s and Y_{ij}'s are Log-normally distributed, one can easily verify that the sampling distribution of t_i^2 is given by

$$\frac{\nu - q - 1}{\nu q} t_i^2 \overset{\text{ind}}{\sim} F_{q,\nu-q-1,\lambda_i}$$

where $\nu = n_x + n_y - 2$ is a degrees of freedom parameter (Johnson & Wichern 2007) (recall that $q = N(N+1)/2$). Note that we make the assumption that the covariance matrices for the two groups are the same, i.e. $\Sigma_i^{(1)} = \Sigma_i^{(2)} = \Sigma_i$. Similar results can be obtained for the unequal covariance case, but with more complicated expressions for the T^2 statistics and the degrees of freedom parameters. The λ_i's are the non-centrality parameters for the non-central F distribution and are given by

$$\lambda_i = \left(\frac{1}{n_x} + \frac{1}{n_y}\right)\left(\widetilde{M_i^{(1)}} - \widetilde{M_i^{(2)}}\right)^T \Sigma_i^{-1} \left(\widetilde{M_i^{(1)}} - \widetilde{M_i^{(2)}}\right).$$

These non-centrality parameters can be interpreted as the (squared) differences between $M_i^{(1)}$ and $M_i^{(2)}$, and they are the parameters we would like to estimate using the statistics (14) computed from the data. Then, based on the estimates $\hat{\lambda}_i$, we select those i's with large estimates, say the largest 1% of all $\hat{\lambda}_i$. However, the process of selection from the computed estimates introduces a *selection bias* (Dawid 1994). The selection bias comes from the fact that it is possible to select some indices i's for which the actual λ_i's are not large but the random errors are large, so that the estimates $\hat{\lambda}_i$ are pushed away from the true parameters λ_i. There are several ways to correct this selection bias, and Efron (2011) proposed to use *Tweedie's formula* for such a purpose.

Tweedie's formula was first proposed by Robbins (1956), and we review this formula here in the context of the classical normal means problem, which is stated as follows. We observe $Z_i \overset{\text{ind}}{\sim} N(\mu_i, \sigma^2)$, $i = 1, \ldots, p$, where the μ_i's are unknown and σ^2 is known, and the goal is to estimate the μ_i's. In the empirical Bayes approach to this problem we assume that μ_i's are iid according to some distribution G. The marginal density of the Z_i's is then

$f(z) = \int \phi_\sigma(z-\mu)\, dG(\mu)$, where ϕ_σ is the density of the $N(0,\sigma^2)$ distribution. With this notation, if G is known (so that f is known), the best estimator of μ_i (under squared error loss) is the so-called Tweedie estimator given by

$$\hat{\mu}_i = Z_i + \sigma^2 \frac{f'(Z_i)}{f(Z_i)}.$$

A feature of this estimator is that it depends on G only through f, and this is desirable because it is fairly easy to estimate f from the Z_i's (so we don't need to specify G). Another interesting observation about this estimator is that $\hat{\mu}_i$ is shrinking the MLE $\hat{\mu}_i^{\text{MLE}} = Z_i$ and can be viewed as a generalization of the James-Stein estimator, which assumes $\mu_i \overset{\text{iid}}{\sim} N(0,\lambda)$ with unknown λ. The Tweedie estimator can be generalized to exponential families. Suppose that $Z_i|\eta_i \overset{\text{ind}}{\sim} f_{\eta_i}(z) = \exp(\eta_i z - \phi(\eta_i)) f_0(z)$, and the prior for ϕ is G. Then the Tweedie estimator for η_i is

$$\hat{\eta}_i = l'(Z_i) - l_0'(Z_i),$$

where $l(z) = \log \int f_\eta(z)\, dG(\eta)$ is the log of the marginal likelihood of the Z_i's and $l_0(z) = \log f_0(z)$.

Although this formula is elegant and useful, it applies only to exponential families. Recently, Du & Hu (2019) derived a Tweedie-type formula for non-central χ^2 statistics, for situations where one is interested in estimating the non-centrality parameters. Suppose $Z_i|\lambda_i \overset{\text{ind}}{\sim} \chi^2_{\nu,\lambda_i}$ and $\lambda_i \overset{\text{iid}}{\sim} G$. Then,

$$E(\lambda_i|Z_i) = \Big[(Z_i - \nu + 4) + 2Z_i\Big(\frac{2l_\nu''(Z_i)}{1+2l_\nu'(Z_i)} + l_\nu'(Z_i)\Big)\Big]\big(1+2l_\nu'(Z_i)\big), \tag{15}$$

where $l_\nu(\cdot)$ is the marginal log-likelihood of the Z_i's (see Theorem 1 in Du & Hu (2019)).

For our situation, if we define $Z_i = [(\nu-q-1)/\nu q]t_i^2$, then

$$Z_i|\lambda_i \overset{\text{ind}}{\sim} F_{q,\nu-q-1,\lambda_i}$$

(recall that $\nu = n_x + n_y - 2$). Assume that the λ_i's are iid according to some distribution G. We would now like to address the problem of how to obtain an empirical Bayes estimate of λ_i. Let $\Phi_{\nu_1,\nu_2,\lambda}$ be the cumulative distribution function (cdf) of the non-central F distribution, $F_{\nu_1,\nu_2,\lambda}$, and let $\tilde{\Phi}_{\nu,\lambda}$ be the cdf of the non-central χ^2 distribution, $\chi^2_{\nu,\lambda}$. Then the transformed variable $Y_i = \tilde{\Phi}^{-1}_{\nu_1,\lambda_i}(\Phi_{\nu_1,\nu_2,\lambda_i}(Z_i))$ follows a non-central χ^2 distribution with degrees of freedom

parameter ν_1 and non-centrality parameter λ_i, and we note that when ν_2 is large, $\Phi_{\nu_1,\nu_2,\lambda_i}$ and $\tilde{\Phi}_{\nu_1,\lambda_i}$ are nearly equal, so that this quantile transformation is nearly the identity. However, the transformation depends on λ_i, which is the parameter to be estimated, so we propose the following iterative algorithm for estimating $E(\lambda_i|Z_i)$. Let $\lambda_i^{(t)}$ be the estimate of λ_i at the t-th iteration. Then, our iterative update of λ_i is given by

$$\lambda_i^{(t+1)} = \Big[(Y_i^{(t)} - \nu_1 + 4) + 2Y_i^{(t)}\Big(\frac{2l''_{\nu_1}(Y_i^{(t)})}{1 + 2l'_{\nu_1}(Y_i^{(t)})} + l'_{\nu_1}(Y_i^{(t)})\Big)\Big]\big(1 + 2l'_{\nu_1}(Y_i^{(t)})\big),$$

where $Y_i^{(t)} = \tilde{\Phi}^{-1}_{\nu_1,\lambda_i^{(t)}}\big(\Phi_{\nu_1,\nu_2,\lambda_i^{(t)}}(Z_i)\big)$, $\nu_1 = q$, and $\nu_2 = \nu - q - 1$. Now the marginal log-likelihood $l_{\nu_1}(y)$ is not available since the prior G for λ_i is unknown. There are several ways to estimate the marginal density of the $Y_i^{(t)}$'s. One of these is through kernel density estimation. However, the iterative formula involves the first and second derivatives of the marginal log-likelihood, and estimates of the derivatives of a density produced through kernel methods are notoriously unstable (see Chapter 3 of Silverman (1986)). There exist different approaches to deal with this problem (see Sasaki et al. (2016) and Shen & Ghosal (2017)). Here we follow Efron (2011) and postulate that l_{ν_1} is well approximated by a polynomial of degree K, and write $l_{\nu_1}(y) = \sum_{k=0}^{K} \beta_k y^k$. The coefficients β_k, $k = 1, \ldots, K$, can be estimated via *Lindsey's method* (Efron & Tibshirani 1996), which is a Poisson regression technique for (parametric) density estimation; the coefficient β_0 is determined by the requirement that $f_{\nu_1}(y) = \exp(l_{\nu_1}(y))$ integrates to 1. The advantage of Lindsey's method over methods that use kernel density estimation is that it does not require us to estimate the derivatives separately, since $l'_{\nu_1}(y) = \sum_{k=1}^{K} k\beta_k y^{k-1}$ and $l''_{\nu_1}(y) = \sum_{k=2}^{K} k(k-1)\beta_k y^{k-2}$. In our experience, with l'_{ν_1} and l''_{ν_1} estimated in this way, if we initialize the scheme by setting $\lambda_i^{(0)}$ to be the estimate of λ_i given by Du & Hu (2019) procedure, then the algorithm converges in less than 10 iterations.

4 Experimental Results

In this section, we describe the performance of our methods on two synthetic data sets and on two sets of real data acquired using diffusion magnetic resonance brain scans of normal (control) subjects and patients with Parkinson disease (PD). For the synthetic data

experiments, we show that (i) the proposed shrinkage estimator for the FM (SURE.Full-FM; *with* simultaneous estimation of the covariance matrices) outperforms the sample FM based on both the Log-Euclidean metric (FM.LE) and the GL-invariant metric (FM.GL) and the shrinkage estimator proposed by Yang & Vemuri (2019) (SURE-FM; *with fixed* covariance matrices) (section 4.1.1) and (ii) the shrinkage estimates of the differences capture the regions that are significantly different between two groups of SPD matrix-valued images (section 4.1.2). For the real data experiments, we demonstrate that (iii) the SURE.Full-FM provides improvement over the three competing estimators (FM.LE, FM.GL, and SURE-FM) for computing an atlas (templates) of diffusion tensor images acquired from human brains (section 4.2.1) and (iv) the proposed shrinkage estimator for detecting group differences is able to identify the regions that are different between patients with PD and control subjects (section 4.2.2). Details of these experiments will be presented subsequently.

4.1 Synthetic Data Experiments

We present two synthetic data experiments here to show that the proposed shrinkage estimator, SURE.Full-FM, outperforms the sample FMs and SURE-FM and that the shrinkage estimates of the group differences can accurately localize the regions that are significantly different between the two groups.

4.1.1 Comparison Between SURE.Full-FM and Competing Estimators

Using synthesized noisy SPD fields (P_3) as data, here we present performance comparisons of four estimators of $\boldsymbol{M}$: (i) SURE.Full-FM, which is the proposed shrinkage estimator, (ii) SURE-FM proposed by Yang & Vemuri (2019) which assumes known covariance matrices, (iii) the MLE, which is denoted by FM.LE, since by proposition 1 it is the FM based on the Log-Euclidean metric, and (iv) the sample FM computed using the GL-invariant metric (using the recursive algorithm in Ho et al. (2013)), denoted by FM.GL. The synthetic data are generated according to (11). Specifically, we set $\mu = I_3$, $\Psi = I_6$, and $n = 10$, and we vary the variance λ and the degree of freedom ν of the prior distribution as follows: $\lambda = 10, 50$, and $\nu = 15, 30$. Figure 1 depicts the relationship between the average loss (averaged over

$m = 1000$ replications) and the dimension p under varying conditions for the four estimators. Note that since the covariance matrices Σ_i's are unknown in our synthetic experiment and $(n-1)^{-1}S_i$ is an unbiased estimate for Σ_i, the A_i's in (10) can be unbiasedly estimated by $[(n-1)q]^{-1}\operatorname{tr} S_i$.

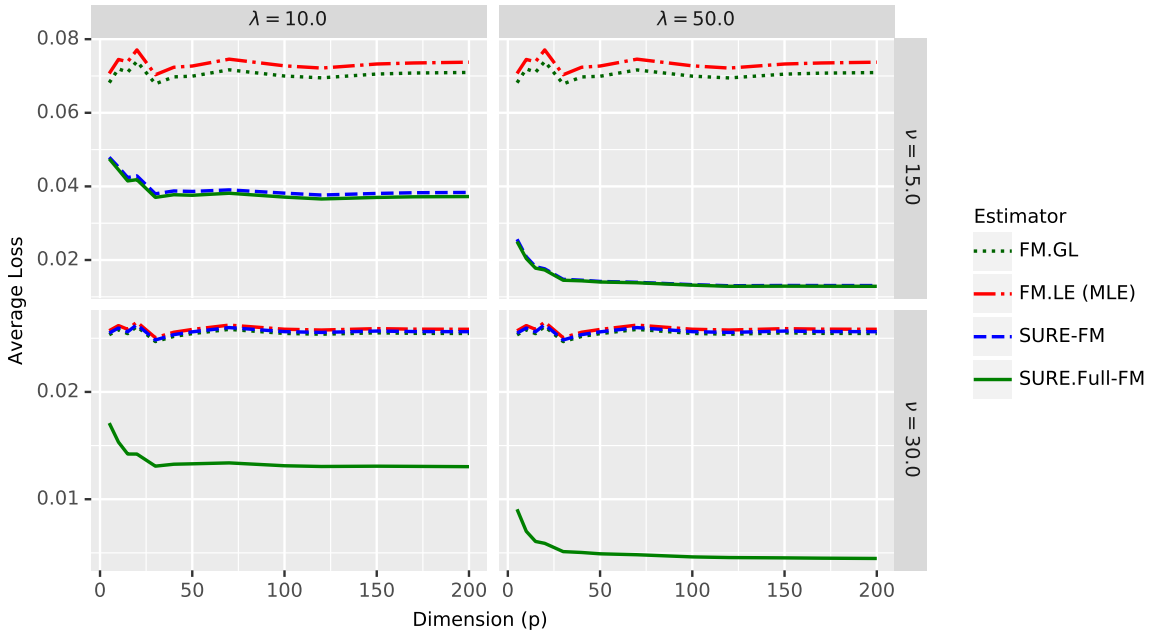


Figure 1: Average loss for the four estimators. Results for varying λ and degree of freedom ν are shown across the columns and rows, respectively. Note that in the bottom two panels, the line corresponding to FM.GL is essentially the same as the FM.LE and SURE.FM, but is barely visible.

As is evident from Figure 1, for large λ the gains from using SURE.Full-FM are greater. This observation is in accordance with our intuition, which is that for large λ, the M_i's are clustered, and it is beneficial to shrink the MLEs of the M_i's towards a common value. The main difference between SURE-FM and SURE.Full-FM is that the former requires knowledge of the Σ_i's and in general such information is not available, and estimates for the Σ_i's are needed to compute the SURE-FM. Hence the performance of SURE-FM depends heavily on how good the estimates for the Σ_i's are. In our synthetic data experiment, we consider the unbiased estimate $\hat{A}_i = [(n-1)q]^{-1}\operatorname{tr} S_i$ for SURE-FM. In this case, the prior mean for Σ_i is $E(\Sigma_i) = (\nu - q - 1)^{-1} I_q$ for which the assumption $\Sigma_i = A_i I$ seems reasonable. For large ν,

the $\hat{A}_i$'s are closer to zero, which results in a smaller shrinkage effect (this can be observed in Figure 1, where we see that SURE-FM is almost identical to FM.LE for $\nu = 30$). *Note that even if the assumption $\Sigma_i = A_i I$ is not severely violated, our estimator still outperforms SURE-FM by a large margin.*

On the other hand, we can fix λ and ν to see how different choices of μ and Ψ affect the performance of our shrinkage estimator SURE.Full-FM. To do this, we fix $n = 10$, $\lambda = 10$, and $\nu = 15$ (so that we can compare with the top-left panel of Figure 1). We consider $\mu = \text{diag}(2, 0.5, 0.5)$ and $\Psi_{ij} = 0.5^{|i-j|}$. The result is shown in Figure 2. The top-left panel of Figure 1 shows that when $\mu = I$ and $\Psi = I$, there is no difference between SURE-FM and SURE.Full-FM, but Figure 2 shows that when one of μ and Ψ is not identity, our shrinkage estimator outperforms SURE-FM. For different choices of λ and ν, the improvement will be more significant, following the trend we observed in Figure 1.

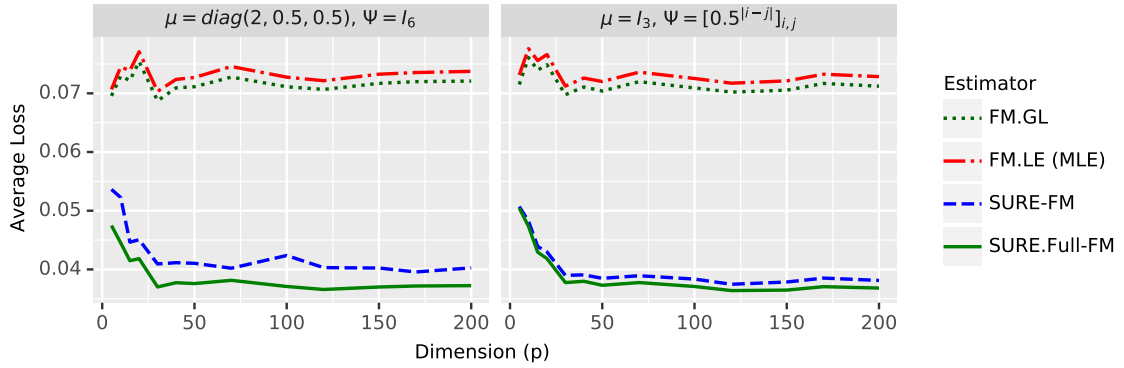


Figure 2: Average losses for the four estimators. The left panel assumes $\mu = \text{diag}(2, 0.5, 0.5)$ and $\Psi = I$ and the right panel assumes $\mu = I$ and $\Psi_{ij} = 0.5^{|i-j|}$.

4.1.2 Differences Between Two Groups of SPD-Valued Images

In this subsection, we demonstrate the method proposed in section 3.3 for evaluating the difference between two groups of SPD-valued images. For this synthetic data experiment, we use P_2, the manifold of 2×2 SPD matrices, since it is easy to visualize these matrices. For the visualization, we represent each 2×2 SPD matrix of the SPD-valued image by an ellipse with the two eigenvectors as the axes of the ellipse and the two eigenvalues as the

width and height along the corresponding axes respectively. The data are synthesized as follows. Given n_k, $M_i^{(k)}$, σ_i^2, $k = 1, 2$, $i = 1, \ldots, p$, generate

$$X_{ij} \overset{\text{ind}}{\sim} \text{LN}(M_i^{(1)}, \sigma_i^2 I), \quad j = 1, \ldots, n_1,$$
$$Y_{ij} \overset{\text{ind}}{\sim} \text{LN}(M_i^{(2)}, \sigma_i^2 I), \quad j = 1, \ldots, n_2.$$

We generate $n_1 = n_2 = 30$ P_2-valued images for the two groups, and the size of each P_2-valued image is 20×20, which gives $p = 20 \times 20 = 400$. For the variances σ_j, we consider a low variance scenario $\sigma_j \overset{\text{iid}}{\sim} U(0.1, 0.3)$ and a high variance scenario $\sigma_j \overset{\text{iid}}{\sim} U(0.3, 0.8)$. The means $M_i^{(k)}$ are depicted visually in Figure 3 (in the form of images with ellipses instead of gray values at each pixel), and the region in which the means are different is the top-right corner, containing a quarter of the pixels; this is the 'ground truth' data.



(a) Group 1 (b) Group 2

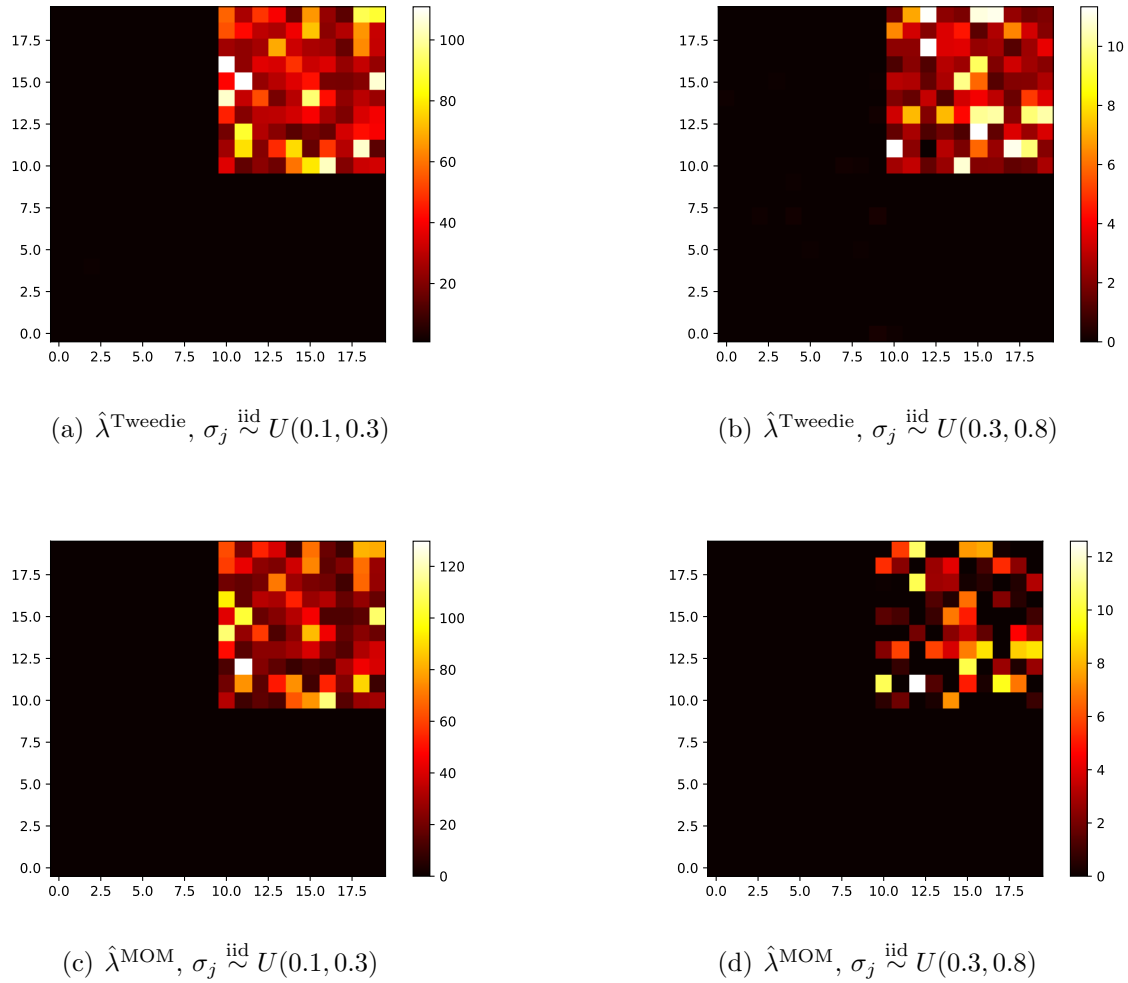
Figure 3: The mean P_2-valued images $M_i^{(k)}$, $k = 1, 2$ used to generate random P_2-valued images for the two groups. The vertical ellipse represents the matrix $\text{diag}(0.2, 1)$ and the horizontal ellipse represents the matrix $\text{diag}(1, 0.2)$.

As described in section 3.3, we first compute the Hotelling T^2 statistic from $\{X_{ij}\}_{j=1}^{n_1}$ and $\{Y_{ij}\}_{j=1}^{n_2}$ for each j and transform each of them to the F statistic. Now we have p non-central F statistics, $f_j \overset{\text{ind}}{\sim} F_{\nu_1, \nu_2, \lambda_j}$, $j = 1, \ldots, p$, where $\nu_1 = q = 3$, and $\nu_2 = n_1 + n_2 - 2 - q - 1 = n_1 + n_2 - 6$. With the resulting F statistics, we can apply the algorithm described in section 3.3 to estimate the non-centrality parameters (at each location), and for the estimation of the marginal log likelihood, we adopt Lindsey's method to fit a polynomial of degree $K = 5$ to the

log-likelihood l_{ν_1}. We have experimented using different values of K, and we found that the results are robust to changes in K, at least for relatively small K. In our experiments, we set $n_1 = n_2 = 30$. As we can see from Figure 3, we expect the method to yield large values on the top-right corner of the image and small values for the rest of the matrix-valued image (field). We compare the proposed estimator $\hat{\lambda}_j^{\text{Tweedie}}$ to the estimator $\hat{\lambda}_j^{\text{MOM}} = \max\left(\frac{\nu_1(\nu_2-2)}{\nu_2} f_j - \nu_1, 0\right)$, which is obtained by the method of moments (MOM) and truncated at 0, and also compare them for different σ_j^2's. Note that we choose to compare with the MOM estimator instead of the MLE for two reasons: (i) the MLE for the non-centrality parameter of non-central F distribution is expensive to compute, and (ii) the MOM is commonly used as a standard for comparison, see for example Kubokawa et al. (1993). As we can see from the results, the Tweedie-adjusted estimator allows us to capture the true region of difference better than the MOM estimator does, and this is especially true for large σ_j^2's. This is due to the presence of the shrinkage effect in Tweedie's formula.

4.2 Real Data Experiments

In this section, we present two real data experiments involving diffusion magnetic resonance image (dMRI) data sets. The diffusion MRI data used here is available for public access via `https://pdbp.ninds.nih.gov/our-data`. dMRI is a diagnostic imaging technique that allows one to non-invasively probe the axonal fiber connectivity in the body by making the magnetic resonance (MR) signal sensitive to water diffusion through the tissue being imaged. In dMRI, the water diffusion is fully characterized by the probability density function (PDF) of the displacement of water molecules, called the ensemble average propagator (EAP) (Callaghan 1993). A simple model that has been widely used to describe the displacement of water molecules is a zero mean Gaussian; its covariance matrix defines the diffusion tensor and characterizes the diffusivity functional locally. The diffusion tensors are 3×3 SPD matrices and hence have 6 unique entries that need to be determined. Thus, the diffusion imaging technique employed in this case involves the application of at least 6 diffusion sensitizing magnetic gradients for acquisition of full 3D MR images (Basser et al. 1994). This dMRI technique is called diffusion tensor imaging (DTI). Some practical techniques for estimating the diffusion tensors and population mean of diffusion tensors accurately can



(a) $\hat{\lambda}^{\text{Tweedie}}$, $\sigma_j \overset{\text{iid}}{\sim} U(0.1, 0.3)$

(b) $\hat{\lambda}^{\text{Tweedie}}$, $\sigma_j \overset{\text{iid}}{\sim} U(0.3, 0.8)$

(c) $\hat{\lambda}^{\text{MOM}}$, $\sigma_j \overset{\text{iid}}{\sim} U(0.1, 0.3)$

(d) $\hat{\lambda}^{\text{MOM}}$, $\sigma_j \overset{\text{iid}}{\sim} U(0.3, 0.8)$

Figure 4: Comparison between the proposed shrinkage estimates and MOM estimates of the non-centrality parameters.

be found in Wang & Vemuri (2004), Chefd'Hotel et al. (2004), Fletcher & Joshi (2004), Alexander (2005), Zhou et al. (2008), Lenglet et al. (2006), and Dryden et al. (2009).

DTI has been the de facto non-invasive dMRI diagnostic imaging technique of choice in the clinic for a variety of neurological ailments. After fitting/estimating the diffusion tensors at each voxel, scalar-valued or vector-valued measures are derived from the diffusion tensors for further analysis. For instance, fractional anisotropy (FA) is a scalar-valued function of the eigenvalues of the diffusion tensor and it was found that FA was reduced in the neuro-anatomical structure called the Substantia Nigra in patients with PD compared to control subjects (Vaillancourt et al. 2009). In Schwartzman et al. (2008), the authors proposed to

use the principal direction, which is the eigenvector corresponding to the largest eigenvalue of the diffusion tensor, to represent the entire tensor; the principal direction contains directional information that any scalar measures such as the FA does not and hence, might be able to capture some subtle differences in the anatomical structure of the brain. In this work, we use the full diffusion tensor which captures both the eigen-values and eigen-vectors, in order to assess the changes caused by pathologies to the underlying tissue micro-architecture revealed via dMRI.

4.2.1 Estimation of the Motor Sensory Tracts of Patients with PD

In this section, we demonstrate the performance of SURE.Full-FM on the dMRI scans of human brain data acquired from 50 patients with PD and 44 control (normal) subjects (CON). The diffusion MRI acquisition parameters were as follows: repetition time = 7748ms, echo time = 86ms, flip angle = 90°, number of diffusion gradients = 64, field of view = 224×224 mm, in-plane resolution = 2 mm isotropic, slice-thickness = 2 mm, and SENSE factor = 2. All the dMRI data were pre-registered into a common coordinate frame prior to any further data processing.

The motor sensory area fiber tracts (M1 fiber tracts) are extracted from each patient of the two groups (PD and CON) using the FSL software (Behrens et al. 2007). The size (length) of each tract is 33 voxels for the left hemisphere tract and 34 voxels for the right hemisphere tract, respectively. Diffusion tensors are then fitted to each of the voxels along each of the tracts to obtain 33 (34) 3×3 SPD matrices. We then compute the Log-Euclidean FM tract for each group (CON and PD). The FM tract here also has 33 (34) diffusion tensors along the tract. We will use these FMs computed from the full population of each group as the 'ground truth'; thus, the underlying distribution in this experiment is the empirical distribution formed by the observed data, i.e. the 33 (34) SPD matrices. Then, we randomly draw a subsample of size $n = 10, 20, 50, 100$ (with replacement) respectively from each group (PD and CON) and compute the SURE.Full-FM (our proposed estimator) and the three competing estimators (FM.LE, FM.GL, and SURE-FM respectively) of each group for each subsample size n. We compare the performance of the different estimators by the distance (using the Log-Euclidean metric) between the estimator and the 'ground truth'

FMs. The entire procedure is repeated for $m = 100$ random draws of subsamples and the average distances are reported in Table 1. Since our proposed shrinkage estimator jointly estimates the FM and the covariance matrices, we also compare our covariance estimates, denoted SURE.Full-Cov, with the MLE of the covariance matrices, i.e., the sample covariance matrices. The results are shown in Table 2.

Table 1: Average loss for the four estimators in estimating the population FM for varying n (with the standard errors in parentheses).

n	10	20	50	100
FM.LE	0.774 (0.03)	0.405 (0.01)	0.159 (0.005)	0.079 (0.002)
FM.GL	0.758 (0.03)	0.396 (0.01)	0.158 (0.004)	0.080 (0.002)
SURE-FM	0.772 (0.03)	0.404 (0.01)	0.160 (0.005)	0.079 (0.002)
SURE.Full-FM	**0.199 (0.01)**	**0.151 (0.003)**	**0.094 (0.002)**	**0.057 (0.001)**

Table 2: Average loss for the two estimators, MLE and SURE.Full-Cov, in estimating the population covariance matrices for varying n (with the standard errors in parentheses).

n	10	20	50	100
MLE	123.69 (5.71)	66.80 (2.69)	25.54 (0.91)	12.91 (0.41)
SURE.Full-Cov	**78.77 (3.21)**	**52.02 (2.03)**	**22.81 (0.80)**	**12.15 (0.38)**

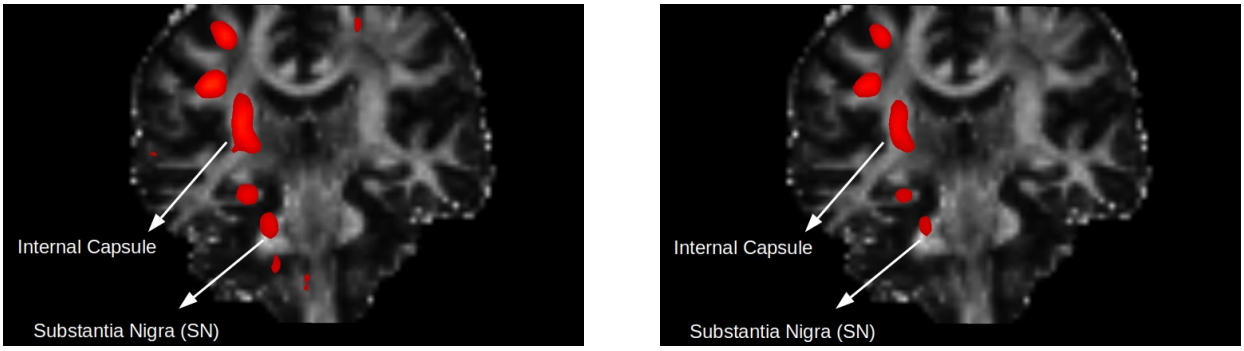
As is evident from Table 1, the SURE.Full-FM outperforms the competing estimators under varying size of subsamples. Also note that, as the sample size increases, the improvement is less significant, which is consistent with the observations on the synthetic data experiments in section 4.1. Recall that in section 4.1.1, the SURE.FM and the SURE.Full-FM perform equally well when the assumption $\Sigma_i = A_i I$ is not violated severely. For real data, it is impossible to check this assumption and it is unlikely to be true. Hence, in this real data experiment, SURE.Full-FM outperforms SURE-FM by a large margin. The improvement of the proposed shrinkage estimator for the covariance matrices over the MLEs is evident from Table 2.

4.2.2 Tweedie-Adjusted Estimator as an Imaging Biomarker

Finally, we apply the shrinkage estimator proposed in section 3.3 to identify the regions that are significantly distinct in diffusional properties (as captured via diffusion tensors) between PD patients and control subjects. In this experiment, the dataset consists of diffusion tensor images (DTIs) of 46 patients with PD and 24 control subjects. To identify the differences between the two groups, we use the diffusion tensor image of the whole brain, which contains $112 \times 112 \times 60$ voxels, without pre-selecting any region of interest. The diffusion tensors are fitted at each voxel across the whole brain volume. The goal of this experiment is to see if we are able to automatically identify the regions capturing the large differences between the PD and control groups and qualitatively validate our findings against what is expected by expert neurologists. In this context, Prodoehl et al. (2013) observed that the region most affected by Parkinson's disease is the Substantia Nigra, which is contained in the Basal Ganglia region of the human brain.

After computing both the Tweedie-adjusted estimates and the MOM estimates of the non-centrality parameters, we select voxels with the largest 1% estimates of the non-centrality parameters and mark those voxels in bright red. (Note that there are other ways to determine the threshold for the selection, for example by using the false discovery rate (FDR) in hypothesis testing problems. However, this is beyond the scope of this paper and we refer the reader to Schwartzman et al. (2008) for interesting work on FDR analysis for DTI datasets.) These voxels are where the large differences between PD and controls are observed. The results are shown in Figure 5. Note that, to take into account the spatial structure, we apply a $4 \times 4 \times 4$ average mask to smooth the result. From the results, we can see that the shrinkage effect of our Tweedie-adjusted estimate successfully corrects the selection bias and produces more accurate identification of the affected regions. Our method is able to capture the Substantia Nigra, which is the region known to be affected by Parkinson's disease. *Notably, our method did not point to the apparently spurious and isolated regions selected by the MOM estimator (the tiny red spots in Figure 5(a)).* We also mention that the past research using FA-based analysis did not report the Internal Capsule as a region affected by Parkinson's disease. We suspect that this discrepancy is due to the fact that FA discards the directional

information of the diffusion tensors while we use the full diffusion tensor which contains the directional information. We plan to conduct a large-scale experiment in our future work to see if this observation continues to hold.



(a) MOM estimates

(b) Tweedie-adjusted estimates

Figure 5: Differences between PD and control groups are superimposed on dMRI scans of a randomly-chosen PD patient and indicated in red.

5 Conclusions

In this work, we presented shrinkage estimators for the mean and covariance of the Log-Normal distribution defined on the manifold P_N of $N \times N$ SPD matrices. We also showed that the proposed shrinkage estimators are asymptotically optimal in a large class of estimators including the MLE. The proposed shrinkage estimators are in closed form and resemble (in form) the James-Stein estimator in Euclidean space $\mathbb{R}^p$. We demonstrated that the proposed shrinkage estimators outperform the MLE via several synthetic data examples and real data experiments using diffusion MRI datasets. The improvements of the proposed shrinkage estimators are significant especially in the small sample size scenarios, which is very pertinent to medical imaging applications.

Our work reported here is however based on the Log-Euclidean metric, and one of the drawbacks of this metric is that it is not affine (GL) invariant, which is a desired property in some applications. Unfortunately, the derivation of the shrinkage estimators under the GL-invariant metric is challenging due to the fact that there is no closed-form expression for some elementary quantities such as the sample FM which makes it almost impossible to

derive the corresponding SURE. Our future research efforts will focus on developing a general framework for designing shrinkage estimators that are applicable to general Riemannian manifolds.

For applications in localizing the regions of the brain where the two groups differ, our approach already works well, but it can potentially be improved if we take into account the fact that neighboring voxels within a region are close under some measure of similarity. For instance, $M_i^{(k)}$ and $M_j^{(k)}$ should be close if voxels i and j are close. This improvement can be achieved by imposing regularization constraints in the proposed framework. However, the ensuing analysis becomes rather complicated and will be the focus of our future efforts.

Supplement to "An Empirical Bayes Approach to Shrinkage Estimation on the Manifold of Symmetric Positive-Definite Matrices"

Abstract

In this supplement, we provide the technical details in section 3.2 of the main paper, including the derivation of the risk function and the SURE, the proofs for Theorem 3 and 4, and the implementation details for minimizing SURE. The notation used in this supplement is the same as in the main paper.

1 Preliminary

Before presenting the proofs, we review the following elementary results for both multivariate normal distributions and Wishart distributions which are use extensively in the proofs. Let $X \sim N_p(\mu, \Sigma)$. Then

$$E\|X - c\|^2 = \operatorname{tr}\Sigma + \|\mu - c\|^2$$
$$E\|X - c\|^4 = (\operatorname{tr}\Sigma)^2 + 2\operatorname{tr}(\Sigma^2) + 4(\mu - c)^T\Sigma(\mu - c) + 2\|\mu - c\|^2\operatorname{tr}\Sigma + \|\mu - c\|^4$$

where $c \in \mathbb{R}^p$. For $X \sim \mathrm{LN}(M, \Sigma)$,

$$Ed^2_{\mathrm{LE}}(X, C) = \operatorname{tr}\Sigma + d^2_{\mathrm{LE}}(M, C)$$
$$Ed^4_{\mathrm{LE}}(X, C) = (\operatorname{tr}\Sigma)^2 + 2\operatorname{tr}(\Sigma^2) + 4(\widetilde{M} - \widetilde{C})^T\Sigma(\widetilde{M} - \widetilde{C}) + 2d^2_{\mathrm{LE}}(M, C)\operatorname{tr}\Sigma + d^4_{\mathrm{LE}}(M, C)$$

where $C \in P_N$. These results can be easily obtained from the definition of the Log-Normal distribution.

Let Y be a $p \times p$ symmetric matrix with eigenvalues $\lambda_1, \ldots, \lambda_p$ and let $\kappa = (k_1, \ldots, k_p)$ be a (non-increasing) partition of a positive integer k, i.e. $k_1 \geq k_2 \geq, \ldots, \geq k_p$ and $\sum_{i=1}^p k_i = k$ where the k_i's are non-negative integers. The *zonal polynomial* of Y corresponding to κ, denoted by $C_\kappa(Y)$, is a symmetric, homogeneous polynomial of degree k in the eigenvalues $\lambda_1, \ldots, \lambda_p$. One of the properties of the zonal polynomials is that $\left(\operatorname{tr} Y\right)^k = \sum_\kappa C_\kappa(Y)$. For

a more precise definition of the zonal polynomial and its calculations, we refer the readers to Ch. 7 of Muirhead (1982). The following lemma is essential in our work.

Lemma 1 *(Muirhead (1982), Corollary 7.2.4) If Y is positive definite, then $C_\kappa(Y) > 0$ for all partitions κ.*

The jth *elementary symmetric function* of Y, denoted by $\mathrm{tr}_j\, Y$, is the sum of all principal minors of order j of the matrix Y. For the case of $j = 1$, $\mathrm{tr}_1\, Y = \sum_{i=1}^{p} \lambda_i = \mathrm{tr}\, Y$, and for the case of $j = 2$, $\mathrm{tr}_2\, Y = \sum_{i<j} \lambda_i \lambda_j$. The definition gives rise to the following identities which are useful in the proofs

$$(\mathrm{tr}\, Y)^2 = \mathrm{tr}(Y^2) + 2\,\mathrm{tr}_2\, Y \tag{16}$$

$$\begin{aligned}(\mathrm{tr}\, Y)^4 &= (\mathrm{tr}(Y^2))^2 + 4\,\mathrm{tr}(Y^2)\,\mathrm{tr}_2\, Y + 4(\mathrm{tr}_2\, Y)^2 \\ &= \mathrm{tr}(Y^4) + 2\,\mathrm{tr}_2\, Y^2 + 2(\mathrm{tr}_2\, Y)(\mathrm{tr}\, Y)^2 \end{aligned} \tag{17}$$

For $S \sim \mathrm{Wishart}_p(\Sigma, \nu)$, the kth moment, $k = 0, 1, 2, \ldots$ of $\mathrm{tr}\, S$ is given by

$$E(\mathrm{tr}\, S)^k = 2^k \sum_{\kappa} \left(\frac{\nu}{2}\right)_\kappa C_\kappa(\Sigma) \tag{18}$$

where

$$(a)_\kappa = \prod_{i=1}^{p} \left(a - \frac{i-1}{2}\right)_{k_i}$$

is called the *generalized hypergeometric coefficient* and

$$(a)_{k_i} = a(a+1)\ldots(a+k_i-1),\ (a)_0 = 1$$

(Gupta & Nagar (2000), Theorem 3.3.23). Next, we review some elementary results for the Wishart distribution:

$$\begin{aligned} ES &= \nu\Sigma \\ ES^2 &= \nu(\nu+1)\Sigma^2 + \nu(\mathrm{tr}\,\Sigma)\Sigma \\ E\,\mathrm{tr}_k\, S &= \nu(\nu-1)\cdots(\nu-k+1)\,\mathrm{tr}_k\,\Sigma \\ E(\mathrm{tr}\, S)^2 &= \nu(\nu+2)(\mathrm{tr}\,\Sigma)^2 - 4\nu\,\mathrm{tr}_2\,\Sigma = \nu^2(\mathrm{tr}\,\Sigma)^2 + 2\nu\,\mathrm{tr}(\Sigma^2). \end{aligned}$$

These results can be found in Gupta & Nagar (2000)(p. 99 and p. 106).

2 Derivation of the Risk Function and the SURE

Recall that the loss function is $L\big((\widehat{\boldsymbol{M}}, \widehat{\boldsymbol{\Sigma}}), (\boldsymbol{M}, \boldsymbol{\Sigma})\big) = p^{-1}\sum_{i=1}^{p} d^2_{\mathrm{LE}}(\widehat{M}_i, M_i) + p^{-1}\sum_{i=1}^{p} \|\widehat{\Sigma}_i - \Sigma_i\| = L_1(\widehat{\boldsymbol{M}}, \boldsymbol{M}) + L_2(\widehat{\boldsymbol{\Sigma}}, \boldsymbol{\Sigma})$. Write $R\big((\widehat{\boldsymbol{M}}, \widehat{\boldsymbol{\Sigma}}), (\boldsymbol{M}, \boldsymbol{\Sigma})\big) = EL_1(\widehat{\boldsymbol{M}}, \boldsymbol{M}) + EL_2(\widehat{\boldsymbol{\Sigma}}, \boldsymbol{\Sigma}) = R_1(\widehat{\boldsymbol{M}}, \boldsymbol{M}) + R_2(\widehat{\boldsymbol{\Sigma}}, \boldsymbol{\Sigma})$. Then

$$\begin{aligned}
R_1(\widehat{\boldsymbol{M}}, \boldsymbol{M}) &= p^{-1}\sum_{i=1}^{p} E d^2_{\mathrm{LE}}(\widehat{M}_i, M_i) \\
&= p^{-1}\sum_{i=1}^{p} \Big[\frac{n^2}{(\lambda+n)^2} E d^2_{\mathrm{LE}}(\bar{X}_i^{\mathrm{LE}}, M_i) + \frac{\lambda^2}{(\lambda+n)^2} d^2_{\mathrm{LE}}(\mu, M_i)\Big] \\
&= p^{-1}(\lambda+n)^{-2}\sum_{i=1}^{p} \Big[n\mathrm{tr}\Sigma_i + \lambda^2 d^2_{\mathrm{LE}}(\mu, M_i)\Big]
\end{aligned}$$

and

$$\begin{aligned}
R_2(\widehat{\boldsymbol{\Sigma}}, \boldsymbol{\Sigma}) &= p^{-1}\sum_{i=1}^{p}(\nu+n-q-2)^{-2} E\|(\Psi - (\nu-q-1)\Sigma_i) + (S_i - (n-1)\Sigma_i)\|^2 \\
&= p^{-1}\sum_{i=1}^{p}(\nu+n-q-2)^{-2}\Big[E\,\mathrm{tr}(S_i^2) - 2(n-1)E\,\mathrm{tr}(S_i\Sigma_i) + (n-1)^2\,\mathrm{tr}(\Sigma_i^2) \\
&\quad + \mathrm{tr}(\Psi^2) - 2(\nu-q-1)\,\mathrm{tr}(\Psi\Sigma_i) + (\nu-q-1)^2\,\mathrm{tr}(\Sigma_i^2)\Big] \\
&= p^{-1}\sum_{i=1}^{p}(\nu+n-q-2)^{-2}\Big[n(n-1)\,\mathrm{tr}(\Sigma_i^2) + (n-1)(\mathrm{tr}\,\Sigma_i)^2 - 2(n-1)^2\,\mathrm{tr}(\Sigma_i^2) \\
&\quad + (n-1)^2\,\mathrm{tr}(\Sigma_i^2) + \mathrm{tr}(\Psi^2) - 2(\nu-q-1)\,\mathrm{tr}(\Psi\Sigma_i) + (\nu-q-1)^2\,\mathrm{tr}(\Sigma_i^2)\Big] \\
&= p^{-1}\sum_{i=1}^{p}(\nu+n-q-2)^{-2}\Big[\big(n-1+(\nu-q-1)^2\big)\mathrm{tr}(\Sigma_i^2) \\
&\quad - 2(\nu-q-1)\mathrm{tr}(\Psi\Sigma_i) + (n-1)(\mathrm{tr}\Sigma_i)^2 + \mathrm{tr}(\Psi^2)\Big].
\end{aligned}$$

To obtain the SURE for this risk function, we first have to find unbiased estimates of the quantities $\mathrm{tr}\,\Sigma_i$, $d^2_{\mathrm{LE}}(\mu, M_i)$, $\mathrm{tr}(\Sigma_i^2)$, $\mathrm{tr}(\Psi\Sigma_i)$, and $(\mathrm{tr}\,\Sigma_i)^2$. With the results provided in

Section 1, it is easy to verify the following equations:

$$\begin{aligned}
\operatorname{tr}\Sigma_i &= E\big((n-1)^{-1}\operatorname{tr} S_i\big)\\
\operatorname{tr}(\Psi\Sigma_i) &= E\big((n-1)^{-1}\operatorname{tr}(\Psi S_i)\big)\\
(\operatorname{tr}\Sigma_i)^2 &= E\Big(\frac{n(\operatorname{tr} S_i)^2 - 2\operatorname{tr} S_i^2}{(n-1)(n+1)(n-2)}\Big)\\
\operatorname{tr}\Sigma_i^2 &= E\Big(\frac{(n-1)\operatorname{tr} S_i^2 - (\operatorname{tr} S_i)^2}{(n-1)(n+1)(n-2)}\Big)\\
d^2_{\mathrm{LE}}(\mu, M_i) &= E\Big(d^2_{\mathrm{LE}}(\bar{X}_i^{\mathrm{LE}}, \mu) - \frac{\operatorname{tr} S_i}{n(n-1)}\Big).
\end{aligned}$$

Plugging the above unbiased estimates into the risk function we obtain

$$\begin{aligned}
\mathrm{SURE}(\lambda, \Psi, \nu, \mu) = p^{-1}\sum_{i=1}^{p}\Bigg\{ & (\lambda+n)^{-2}\Big[\frac{n}{n-1}\operatorname{tr} S_i + \lambda^2 d^2_{\mathrm{LE}}(\bar{X}_i^{\mathrm{LE}}, \mu) - \frac{\lambda^2}{n(n-1)}\operatorname{tr} S_i\Big]\\
& + (\nu+n-q-2)^{-2}\Big[(n-1+(\nu-q-1)^2)\Big(\frac{(n-1)\operatorname{tr} S_i^2 - (\operatorname{tr} S_i)^2}{(n-1)(n+1)(n-2)}\Big)\\
& + \frac{n(\operatorname{tr} S_i)^2 - 2\operatorname{tr} S_i^2}{(n+1)(n-2)} - 2\frac{\nu-q-1}{n-1}\operatorname{tr}(\Psi S_i) + \operatorname{tr}(\Psi^2)\Big]\Bigg\}\\
= p^{-1}\Bigg\{ & \sum_{i=1}^{p}(\lambda+n)^{-2}\Big[\frac{n-\lambda^2/n}{n-1}\operatorname{tr} S_i + \lambda^2 d^2_{\mathrm{LE}}(\bar{X}_i^{\mathrm{LE}}, \mu)\Big]\\
& + (\nu+n-q-2)^{-2}\Big[\frac{n-3+(\nu-q-1)^2}{(n+1)(n-2)}\operatorname{tr}(S_i^2)\\
& + \frac{(n-1)^2-(\nu-q-1)^2}{(n-1)(n+1)(n-2)}\big(\operatorname{tr} S_i\big)^2 - 2\frac{\nu-q-1}{n-1}\operatorname{tr}(\Psi S_i) + \operatorname{tr}(\Psi^2)\Big]\Bigg\}.
\end{aligned}$$

3 Proofs of the Theorems

The following lemmas are essential for proving the main theorems.

Lemma 2 *(Xie et al. 2012) Let $X_i \overset{ind}{\sim} N(\theta_i, A_i)$. Assume the following conditions:*

(i) $\limsup_{p\to\infty} p^{-1}\sum_{i=1}^{p} A_i^2 < \infty$,

(ii) $\limsup_{p\to\infty} p^{-1}\sum_{i=1}^{p} A_i\theta_i^2 < \infty$,

(iii) $\limsup_{p\to\infty} p^{-1}\sum_{i=1}^{p} |\theta_i|^{2+\delta} < \infty$ *for some* $\delta > 0$.

Then $E\big(\max_{1\le i\le p} X_i^2\big) = O(p^{2/(2+\delta^*)})$ *where* $\delta^* = \min(1, \delta)$.

The next lemma is an extension of the previous lemma to Log-Normal distributions.

Lemma 3 *Let* $X_i \overset{ind}{\sim} LN(M_i, \Sigma_i)$ *on* P_N *and* $q = N(N+1)/2$. *Assume the following conditions:*

(i) $\limsup_{p\to\infty} p^{-1} \sum_{i=1}^{p} \left(\operatorname{tr} \Sigma_i\right)^2 < \infty$,

(ii) $\limsup_{p\to\infty} p^{-1} \sum_{i=1}^{p} \widetilde{M}_i^T \Sigma_i \widetilde{M}_i < \infty$,

(iii) $\limsup_{p\to\infty} p^{-1} \sum_{i=1}^{p} \|\log M_i\|^{2+\delta} < \infty$ *for some* $\delta > 0$.

Then $E\big(\max_{1\le i\le p} \|\log X_i\|^2\big) = O(p^{2/(2+\delta^*)})$ *where* $\delta^* = \min(1, \delta)$.

Proof. Write $Y_i = \widetilde{X}_i$ and $\mu_i = \widetilde{M}_i$. Then $\|Y_i\|^2 = \|\log X_i\|^2$. From the definition of the Log-Normal distribution, $Y_i \overset{\text{ind}}{\sim} N_q(\mu_i, \Sigma_i)$. Since for $j = 1, \ldots, q$

$$\begin{aligned}
\sum_{i=1}^{p} \Sigma_{i,jj}^2 &< \sum_{i=1}^{p} \left(\operatorname{tr} \Sigma_i\right)^2 \\
\sum_{i=1}^{p} \Sigma_{i,jj} \mu_{i,j}^2 &< \sum_{i=1}^{p} \mu_i^T \Sigma_i \mu_i = \sum_{i=1}^{p} \widetilde{M}_i^T \Sigma_i \widetilde{M}_i \\
\sum_{i=1}^{p} |\mu_{i,j}|^{2+\delta} &< \sum_{i=1}^{p} \|\mu_i\|^{2+\delta} = \sum_{i=1}^{p} \|\log M_i\|^{2+\delta},
\end{aligned}$$

by Lemma 2, we have $E(\max_{1\le i\le,p} Y_{i,j}^2) = O(p^{2/(2+\delta^*)})$. Then

$$\begin{aligned}
E\Big(\max_{1\le i\le p} \|\log X_i\|^2\Big) &= E\Big(\max_{1\le i\le p} \|Y_i\|^2\Big) \\
&\le E\Big(\sum_{j=1}^{q} \max_{1\le i\le p} Y_{i,j}^2\Big) = \sum_{j=1}^{q} E\Big(\max_{1\le i\le p} Y_{i,j}^2\Big) = O(p^{2/(2+\delta*)})
\end{aligned}$$

which concludes the proof. □

Lemma 4 *Let* $S_i \overset{ind}{\sim}$ *Wishart*(Σ_i, ν) *where the* Σ_i*'s are* $q \times q$ *symmetric positive-definite matrices. If* $\limsup_{p\to\infty} p^{-1} \sum_{i=1}^{p} (\operatorname{tr} \Sigma_i)^4 < \infty$, *then* $E(\max_{1\le i\le p} \|S_i\|^2) = O(q^2 p^{1/2} (\log p)^2 + q^2 p^{1/2} (\log q)^2)$.

Proof. Write $S_i = X_i X_i^T$ where $X_i \overset{\text{ind}}{\sim} N_q(0, \Sigma_i)$. Then $\|S_i\|^2 = \|X_i\|^4$. From Lemma 2, we have $E(\max_{1\le j\le q} X_{i,j}^2) = O(p^{2/3})$ and $E(\max_{1\le i\le p, 1\le j\le q} X_{i,j}^2) = O(q^{2/3} p^{2/3})$. Let $X_{i,j} = \Sigma_{i,j}^{1/2} Z_{i,j}$ where $Z_{i,j} \overset{\text{iid}}{\sim} N(0,1)$. Then $X_{i,j}^4 = \Sigma_{i,jj}^2 Z_{i,j}$ and

$$\max_{1\le i\le p, 1\le j\le q} X_{i,j}^4 \le \max_{1\le i\le p, q\le j\le q} \Sigma_{i,jj}^2 \cdot \max_{1\le i\le p, 1\le j\le q} Z_{i,j}.$$

Since

$$\max_{1\le i\le p,1\le j\le q}\Sigma_{i,jj}^4 < \max_{1\le i\le p}\mathrm{tr}(\Sigma_i)^4 < \sum_{i=1}^{p}\mathrm{tr}(\Sigma_i)^4 = O(p)$$

implies $\max_{1\le i\le p,1\le j\le q}\Sigma_{i,jj}^2 = O(p^{1/2})$ and

$$E\Big(\max_{1\le i\le p,1\le j\le q} Z_{i,j}^4\Big) = O((\log p+\log q)^2),$$

we have

$$\begin{aligned} E\Big(\max_{1\le i\le p,1\le j\le q} X_{i,j}^4\Big) &\le \max_{1\le i\le p,q\le j\le q}\Sigma_{i,jj}^2 E\Big(\max_{1\le i\le p,1\le j\le q} Z_{i,j}\Big) \\ &= O(p^{1/2}(\log p+\log q)^2). \end{aligned}$$

Then

$$\begin{aligned} E\Big(\max_{1\le i\le p}\|S_i\|^2\Big) = E\Big(\max_{1\le i\le p}\|X_i\|^4\Big) &= E\left[\max_{1\le i\le p}\left(\sum_{j=1}^{q}X_{i,j}^2\right)^2\right] \\ &= E\left[\max_{1\le i\le p}\left(\sum_{j=1}^{q}X_{i,j}^4+\sum_{j\ne k}X_{i,j}^2X_{i,k}^2\right)\right] \\ &\le qE\Big(\max_{1\le i\le p,1\le j\le q}X_{i,j}^4\Big)+q(q-1)E\Big(\max_{1\le i\le p,1\le j\le q}X_{i,j}^4\Big) \\ &\le q^2O(p^{1/2}(\log p+\log q)^2) \\ &= O(q^2p^{1/2}(\log p)^2+q^2p^{1/2}(\log q)^2) \end{aligned}$$

□

Theorem 3 *Assume the following conditions:*

(i) $\limsup_{p\to\infty}p^{-1}\sum_{i=1}^{p}\left(\mathrm{tr}\,\Sigma_i\right)^4<\infty$,

(ii) $\limsup_{p\to\infty}p^{-1}\sum_{i=1}^{p}\widetilde{M}_i^T\Sigma_i\widetilde{M}_i<\infty$,

(iii) $\limsup_{p\to\infty}p^{-1}\sum_{i=1}^{p}\|\log M_i\|^{2+\delta}<\infty$ *for some* $\delta>0$.

Then

$$\sup_{\substack{\lambda>0,\nu>q+1,\|\Psi\|\le\max_{1\le i\le p}\|S_i\|,\\ \|\log\mu\|\le\max_{1\le i\le p}\|\log\bar{X}_i^{LE}\|}}\Big|SURE(\lambda,\Psi,\nu,\mu)-L\Big(\big(\widehat{\boldsymbol{M}}^{\lambda,\mu},\widehat{\boldsymbol{\Sigma}}^{\Psi,\nu}\big),\big(\boldsymbol{M},\boldsymbol{\Sigma}\big)\Big)\Big|\xrightarrow{prob}0\quad as\ p\to\infty.$$

Proof. Note that in this proof, we write $\bar{X}_i^{\mathrm{LE}}$ as $\bar{X}_i$ to simplify the notation. First, we write the loss function L as

$$\begin{aligned} L\Big((\widehat{\boldsymbol{M}}^{\lambda,\mu}, \widehat{\boldsymbol{\Sigma}}^{\Psi,\nu}), (\boldsymbol{M}, \boldsymbol{\Sigma})\Big) &= p^{-1}\sum_{i=1}^{p} d_{\mathrm{LE}}^2(\widehat{M}_i^{\lambda,\mu}, M_i) + \|\widehat{\Sigma}_i^{\Psi,\nu} - \Sigma_i\|^2 \\ &= L_1\Big(\widehat{\boldsymbol{M}}^{\lambda,\mu}, \boldsymbol{M}\Big) + L_2\Big(\widehat{\boldsymbol{\Sigma}}^{\Psi,\nu}, \boldsymbol{\Sigma}\Big), \end{aligned}$$

where

$$\begin{aligned} L_1\Big(\widehat{\boldsymbol{M}}^{\lambda,\mu}, \boldsymbol{M}\Big) &= p^{-1}\sum_{i=1}^{p} \Big\|(\lambda+n)^{-1}\Big(n\Big(\log\bar{X}_i - \log M_i\Big) + \lambda\Big(\log\mu - \log M_i\Big)\Big)\Big\|^2 \\ &= p^{-1}\sum_{i=1}^{p}(\lambda+n)^{-2}\Big[n^2 d_{\mathrm{LE}}^2(\bar{X}_i, M_i) + \lambda^2 d_{\mathrm{LE}}^2(\mu, M_i) \\ &\quad + 2n\lambda\big\langle \log\bar{X}_i - \log M_i, \log\mu - \log M_i\big\rangle\Big], \\ L_2\Big(\widehat{\boldsymbol{\Sigma}}^{\Psi,\nu}, \boldsymbol{\Sigma}\Big) &= p^{-1}\sum_{i=1}^{p}(\nu+n-q-2)^{-2}\Big\|\big(\Psi - (\nu-q-1)\Sigma_i\big) + \big(S_i - (n-1)\Sigma_i\big)\Big\|^2 \\ &= p^{-1}\sum_{i=1}^{p}(\nu+n-q-2)^{-2}\Big[\operatorname{tr}\big(\Psi^2\big) - 2(\nu-q-1)\operatorname{tr}\big(\Psi\Sigma_i\big) + (\nu-q-1)^2\operatorname{tr}\big(\Sigma_i^2\big) \\ &\quad + \operatorname{tr}\big(S_i^2\big) - 2(n-1)\operatorname{tr}\big(S_i\Sigma_i\big) + (n-1)^2\operatorname{tr}\big(\Sigma_i^2\big) \\ &\quad + 2\langle\Psi - (\nu-q-1)\Sigma_i, S_i - (n-1)\Sigma_i\rangle\Big]. \end{aligned}$$

Write the SURE as

$$\mathrm{SURE}(\lambda,\mu,\Psi,\nu) = \mathrm{SURE}_1(\lambda,\mu) + \mathrm{SURE}_2(\Psi,\nu),$$

where

$$\begin{aligned} \mathrm{SURE}_1(\lambda,\mu) &= p^{-1}\sum_{i=1}^{p}(\lambda+n)^{-2}\Big[\frac{n-\lambda^2/n}{n-1}\operatorname{tr} S_i + \lambda^2 d_{\mathrm{LE}}^2(\bar{X}_i,\mu)\Big], \\ \mathrm{SURE}_2(\Psi,\nu) &= p^{-1}\sum_{i=1}^{p}(\nu+n-q-2)^{-2}\Bigg[\frac{n-3+(\nu-q-1)^2}{(n+1)(n-2)}\operatorname{tr}\big(S_i^2\big) \\ &\quad + \frac{(n-1)^2-(\nu-q-1)^2}{(n-2)(n-1)(n+1)}\big(\operatorname{tr} S_i\big)^2 - 2\frac{\nu-q-1}{n-1}\operatorname{tr}\big(\Psi S_i\big) + \operatorname{tr}\big(\Psi^2\big)\Bigg]. \end{aligned}$$

Since

$$\sup_{\substack{\lambda>0,\nu>q+1,\|\Psi\|\le\max_{1\le i\le p}\|S_i\|,\\ \|\log\mu\|\le\max_{1\le i\le p}\|\log\bar{X}_i^{\mathrm{LE}}\|}}\Big|\mathrm{SURE}(\lambda,\Psi,\nu,\mu)-L\Big(\big(\widehat{\boldsymbol{M}}^{\lambda,\mu},\widehat{\boldsymbol{\Sigma}}^{\Psi,\nu}\big),\big(\boldsymbol{M},\boldsymbol{\Sigma}\big)\Big)\Big|\le$$

$$\sup_{\lambda>0,\|\log\mu\|\le\max_{1\le i\le p}\|\log\bar{X}_i\|}\big|\mathrm{SURE}_1(\lambda,\mu)-L_1\big(\widehat{\boldsymbol{M}}^{\lambda,\mu},\boldsymbol{M}\big)\big|$$

$$+\sup_{\nu>q+1,\|\Psi\|\le\max_{1\le i\le p}\|S_i\|}\big|\mathrm{SURE}_2(\Psi,\nu)-L_2\big(\widehat{\boldsymbol{\Sigma}}^{\Psi,\nu},\boldsymbol{\Sigma}\big)\big|,$$

it suffices to show the two terms on the right-hand side converge to 0 in probability. For the first term,

$$\begin{aligned}
|\mathrm{SURE}_1(\lambda,\mu)-L_1\big(\widehat{\boldsymbol{M}}^{\lambda,\mu},\boldsymbol{M}\big)| &= \Bigg|p^{-1}\sum_{i=1}^{p}(\lambda+n)^{-2}\Bigg[\frac{n}{n-1}\operatorname{tr}S_i-n^2d_{\mathrm{LE}}^2(\bar{X}_i,M_i)\\
&\quad+\lambda^2\Big(\frac{\operatorname{tr}S_i}{n(n-1)}+d_{\mathrm{LE}}^2(\bar{X}_i,\mu)-d_{\mathrm{LE}}^2(M_i,\mu)\Big)\\
&\quad+2n\lambda\Big\langle\log\bar{X}_i-\log M_i,\log\mu-\log M_i\Big\rangle\Bigg]\Bigg|\\
&\le\Bigg|p^{-1}\sum_{i=1}^{p}(\lambda+n)^{-2}\Big(\frac{n}{n-1}\operatorname{tr}S_i-n^2d_{\mathrm{LE}}^2(\bar{X}_i,M_i)\Big)\Bigg| \qquad (19)\\
&\quad+\Bigg|p^{-1}\sum_{i=1}^{p}\frac{\lambda^2}{(\lambda+n)^2}\Big(\frac{\operatorname{tr}S_i}{n(n-1)}+d_{\mathrm{LE}}^2(\bar{X}_i,\mu)-d_{\mathrm{LE}}^2(M_i,\mu)\Big)\Bigg| \qquad (20)\\
&\quad+\Bigg|p^{-1}\sum_{i=1}^{p}\frac{2n\lambda}{(\lambda+n)^2}\Big\langle\log\bar{X}_i-\log M_i,\log\mu-\log M_i\Big\rangle\Bigg|. \qquad (21)
\end{aligned}$$

We will now prove the convergence of each of the three terms individually.

For (19), from assumption (i), we have

$$
\begin{aligned}
&\operatorname{Var}\left(p^{-1}\sum_{i=1}^{p}\Big(\frac{n}{n-1}\operatorname{tr} S_i - n^2 d_{\mathrm{LE}}^2(\bar{X}_i, M_i)\Big)\right) \\
&= \frac{1}{p}p^{-1}\sum_{i=1}^{p}\operatorname{Var}\Big(\frac{n}{n-1}\operatorname{tr} S_i - n^2 d_{\mathrm{LE}}^2(\bar{X}_i, M_i)\Big) \\
&= \frac{1}{p}p^{-1}\sum_{i=1}^{p}E\Big(\frac{n}{n-1}\operatorname{tr} S_i - n^2 d_{\mathrm{LE}}^2(\bar{X}_i, M_i)\Big)^2 \\
&= \frac{n^2}{p}p^{-1}\sum_{i=1}^{p}\Big[\frac{E\big(\operatorname{tr} S_i\big)^2}{(n-1)^2} + n^2 E d_{\mathrm{LE}}^4(\bar{X}_i, M_i) - 2\frac{n}{n-1}E\big(\operatorname{tr} S_i\big)E d_{\mathrm{LE}}^2(\bar{X}_i, M_i)\Big] \\
&= \frac{n^2}{p}p^{-1}\sum_{i=1}^{p}\Big[\frac{n+1}{n-1}\big(\operatorname{tr}\Sigma_i\big)^2 + 4\frac{\operatorname{tr}_2\Sigma_i}{n-1} + \big(\operatorname{tr}\Sigma_i\big)^2 + 2\operatorname{tr}\big(\Sigma_i^2\big) - 2\big(\operatorname{tr}\Sigma_i\big)^2\Big] \\
&= \frac{n^2}{p}p^{-1}\sum_{i=1}^{p}\Big[\frac{2}{n-1}\big(\operatorname{tr}\Sigma_i\big)^2 + \frac{4}{n-1}\operatorname{tr}_2\Sigma_i + 2\operatorname{tr}\big(\Sigma_i^2\big)\Big] \overset{p\to\infty}{\longrightarrow} 0.
\end{aligned}
$$

Then, by Markov's inequality,

$$
\left|p^{-1}\sum_{i=1}^{p}\Big(\frac{n}{n-1}\operatorname{tr} S_i - n^2 d_{\mathrm{LE}}^2(\bar{X}_i, M_i)\Big)\right| \xrightarrow{\text{prob}} 0 \quad \text{as } p\to\infty.
$$

Thus

$$
\begin{aligned}
&\sup_{\lambda>0}\left|p^{-1}\sum_{i=1}^{p}(\lambda+n)^{-2}\Big(\frac{n}{n-1}\operatorname{tr} S_i - n^2 d_{\mathrm{LE}}^2(\bar{X}_i, M_i)\Big)\right| \\
&= \Big(\sup_{\lambda>0}(\lambda+n)^{-2}\Big)\left|p^{-1}\sum_{i=1}^{p}\Big(\frac{n}{n-1}\operatorname{tr} S_i - n^2 d_{\mathrm{LE}}^2(\bar{X}_i, M_i)\Big)\right| \\
&= \frac{1}{n^2}\left|p^{-1}\sum_{i=1}^{p}\Big(\frac{n}{n-1}\operatorname{tr} S_i - n^2 d_{\mathrm{LE}}^2(\bar{X}_i, M_i)\Big)\right| \xrightarrow{\text{prob}} 0 \quad \text{as } p\to\infty. \qquad (22)
\end{aligned}
$$

Remark 1 By the identity (16), assumption (i) implies $\limsup_{p\to\infty} p^{-1}\sum_{i=1}^{p}\operatorname{tr}\big(\Sigma_i^2\big) < \infty$ and $\limsup_{p\to\infty} p^{-1}\sum_{i=1}^{p}\operatorname{tr}_2\Sigma_i < \infty$.

For (20),

$$
\begin{aligned}
&\sup_{\lambda>0,\|\log\mu\|\le\max_{1\le i\le p}\|\log\bar{X}_i\|}\left|p^{-1}\sum_{i=1}^{p}\frac{\lambda^2}{(\lambda+n)^2}\Big(\frac{\operatorname{tr}S_i}{n(n-1)}+d^2_{\mathrm{LE}}(\bar{X}_i,\mu)-d^2_{\mathrm{LE}}(M_i,\mu)\Big)\right|\\
&=\sup_{\lambda>0,\|\log\mu\|\le\max_{1\le i\le p}\|\log\bar{X}_i\|}\left|p^{-1}\sum_{i=1}^{p}\frac{\lambda^2}{(\lambda+n)^2}\Big(\frac{\operatorname{tr}S_i}{n(n-1)}+\|\log\bar{X}_i\|^2-\|\log M_i\|^2\right.\\
&\qquad\left.+2\langle\log\bar{X}_i-\log M_i,\log\mu\rangle\Big)\right|\\
&\le\sup_{\lambda>0}\left|p^{-1}\sum_{i=1}^{p}\frac{\lambda^2}{(\lambda+n)^2}\Big(\frac{\operatorname{tr}S_i}{n(n-1)}+\|\log\bar{X}_i\|^2-\|\log M_i\|^2\Big)\right|\\
&\qquad+\sup_{\lambda>0,\|\log\mu\|\le\max_{1\le i\le p}\|\log\bar{X}_i\|}\left|p^{-1}\frac{2\lambda^2}{(\lambda+n)^2}\Big\langle\sum_{i=1}^{p}\log\bar{X}_i-\log M_i,\log\mu\Big\rangle\right|\\
&\le\Big(\sup_{\lambda>0}\frac{\lambda^2}{(\lambda+n)^2}\Big)\left|p^{-1}\sum_{i=1}^{p}\Big(\frac{\operatorname{tr}S_i}{n(n-1)}+\|\log\bar{X}_i\|^2-\|\log M_i\|^2\Big)\right|\\
&\qquad+\sup_{\lambda>0,\|\log\mu\|\le\max_{1\le i\le p}\|\log\bar{X}_i\|}\left|p^{-1}\frac{2\lambda^2}{(\lambda+n)^2}\|\log\mu\|\left\|\sum_{i=1}^{p}\big(\log\bar{X}_i-\log M_i\big)\right\|\right|\\
&\qquad\qquad\qquad\qquad\qquad\qquad\qquad\qquad\qquad\qquad\text{(By Cauchy's inequality)}\\
&\le\left|p^{-1}\sum_{i=1}^{p}\Big(\frac{\operatorname{tr}S_i}{n(n-1)}+\|\log\bar{X}_i\|^2-\|\log M_i\|^2\Big)\right|\\
&\qquad+\left|p^{-1}\max_{1\le i\le p}\|\log\bar{X}_i\|\left\|\sum_{i=1}^{p}\big(\log\bar{X}_i-\log M_i\big)\right\|\right|
\end{aligned}
$$

Since by assumptions (i) and (ii),

$$
\begin{aligned}
&\operatorname{Var}\left(p^{-1}\sum_{i=1}^{p}\Big(\frac{\operatorname{tr} S_i}{n(n-1)}+\|\log\bar{X}_i\|^2-\|\log M_i\|^2\Big)\right)\\
&=p^{-2}\sum_{i=1}^{p}\operatorname{Var}\Big(\frac{\operatorname{tr} S_i}{n(n-1)}+\|\log\bar{X}_i\|^2-\|\log M_i\|^2\Big)\\
&=p^{-2}\sum_{i=1}^{p}E\Big(\frac{\operatorname{tr} S_i}{n(n-1)}+\|\log\bar{X}_i\|^2-\|\log M_i\|^2\Big)^2\\
&=p^{-2}\sum_{i=1}^{p}\Bigg[\left(\frac{n+1}{n^2(n-1)}\big(\operatorname{tr}\Sigma_i\big)^2-\frac{4}{n^2(n-1)}\operatorname{tr}_2\Sigma_i\right)\left(+\frac{\big(\operatorname{tr}\Sigma_i\big)^2}{n^2}+\frac{2\operatorname{tr}\big(\Sigma_i^2\big)}{n^2}\right.\\
&\qquad\left.+\frac{4}{n}\widetilde{M}_i^T\Sigma_i\widetilde{M}_i+\frac{2}{n}\|\log M_i\|^2\operatorname{tr}\Sigma_i+\|\log M_i\|^4\right)+\|\log M_i\|^4\\
&\qquad+\frac{2}{n}\operatorname{tr}\Sigma_i\Big(\frac{1}{n}\operatorname{tr}\Sigma_i+\|\log M_i\|^2\Big)-2\Big(\frac{1}{n}\operatorname{tr}\Sigma_i+\|\log M_i\|^2\Big)\|\log M_i\|^2-\frac{2}{n}\operatorname{tr}\Sigma_i\|\log M_i\|^2\Bigg]\\
&=p^{-2}\sum_{i=1}^{p}\left[\frac{4n-2}{n^2(n-1)}\big(\operatorname{tr}\Sigma_i\big)^2-\frac{4}{n^2(n-1)}\operatorname{tr}_2\Sigma_i+\frac{2}{n}\operatorname{tr}\big(\Sigma_i^2\big)+\frac{4}{n}\widetilde{M}_i^T\Sigma_i\widetilde{M}_i\right]\overset{p\to\infty}{\longrightarrow}0,
\end{aligned}
$$

we have

$$
\left|p^{-1}\sum_{i=1}^{p}\Big(\frac{\operatorname{tr} S_i}{n(n-1)}+\|\log\bar{X}_i\|^2-\|\log M_i\|^2\Big)\right|\overset{\text{prob}}{\longrightarrow}0\quad\text{as } p\to\infty
$$

by Markov's inequality. Since by Lemma 3,

$$
\begin{aligned}
&E\left[\frac{2}{p}\max_{1\le i\le p}\|\log\bar{X}_i\|\left\|\sum_{i=1}^{p}\big(\log\bar{X}_i-\log M_i\big)\right\|\right]\\
&\le\frac{2}{p}\left[E\Big(\max_{1\le i\le p}\|\log\bar{X}_i\|^2\Big)E\left\|\sum_{i=1}^{p}\big(\log\bar{X}_i-\log M_i\big)\right\|^2\right]^{1/2}\\
&=O(p^{-1})\times O(p^{1/(2+\delta^*)})\times O(p^{1/2})\\
&=O(p^{-\delta^*/(4+2\delta^*)}),
\end{aligned}
$$

we have

$$
\sup_{\lambda>0,\|\log\mu\|\le\max_{1\le i\le p}\|\log\bar{X}_i\|}\left|p^{-1}\sum_{i=1}^{p}\frac{\lambda^2}{(\lambda+n)^2}\Big(\frac{\operatorname{tr} S_i}{n(n-1)}+d_{\mathrm{LE}}^2(\bar{X}_i,\mu)-d_{\mathrm{LE}}^2(M_i,\mu)\Big)\right|\overset{\text{prob}}{\longrightarrow}0
$$

$$
\text{as } p\to\infty.\quad(23)
$$

For (21), we have

$$\begin{aligned}
&\sup_{\lambda>0,\|\log\mu\|\le\max_{1\le i\le p}\|\log\bar{X}_i\|}\left|p^{-1}\sum_{i=1}^{p}\frac{2n\lambda}{(\lambda+n)^2}\Big\langle\log\bar{X}_i-\log M_i,\log\mu-\log M_i\Big\rangle\right| \\
&\le\sup_{\lambda>0}\left|p^{-1}\frac{2n\lambda}{(\lambda+n)^2}\max_{1\le i\le p}\|\log\bar{X}_i\|\left\|\sum_{i=1}^{p}\big(\log\bar{X}_i-\log M_i\big)\right\|\right| \\
&\quad+\sup_{\lambda>0}\left|p^{-1}\sum_{i=1}^{p}\frac{2n\lambda}{(\lambda+n)^2}\Big\langle\log\bar{X}_i-\log M_i,\log M_i\Big\rangle\right| \\
&=\left|\frac{1}{2p}\max_{1\le i\le p}\|\log\bar{X}_i\|\left\|\sum_{i=1}^{p}\big(\log\bar{X}_i-\log M_i\big)\right\|\right|+\left|\frac{1}{2p}\sum_{i=1}^{p}\Big\langle\log\bar{X}_i-\log M_i,\log M_i\Big\rangle\right|
\end{aligned}$$

since $\sup_{\lambda>0}2n\lambda/(\lambda+n)^2=1/2$. By assumption (ii), we have

$$\begin{aligned}
&\mathrm{Var}\left[p^{-1}\sum_{i=1}^{p}\Big\langle\log\bar{X}_i-\log M_i,\log M_i\Big\rangle\right] \\
&=p^{-2}\sum_{i=1}^{p}E\Big\langle\log\bar{X}_i-\log M_i,\log M_i\Big\rangle^2 \\
&=p^{-2}\sum_{i=1}^{p}E\widetilde{M}_i^T\left[\Big(\widetilde{\bar{X}}_i-\widetilde{M}_i\Big)\Big(\widetilde{\bar{X}}_i-\widetilde{M}_i\Big)^T\right]\widetilde{M}_i \\
&=p^{-2}\sum_{i=1}^{p}\frac{1}{n}\widetilde{M}_i^T\Sigma_i\widetilde{M}_i\overset{p\to\infty}{\longrightarrow}0
\end{aligned}$$

and again by Markov's inequality,

$$\left|\frac{1}{2p}\sum_{i=1}^{p}\Big\langle\log\bar{X}_i-\log M_i,\log M_i\Big\rangle\right|\overset{\text{prob}}{\longrightarrow}0\quad\text{as } p\to\infty.$$

Thus,

$$\sup_{\lambda>0,\|\log\mu\|\le\max_{1\le i\le p}\|\log\bar{X}_i\|}\left|p^{-1}\sum_{i=1}^{p}\frac{2n\lambda}{(\lambda+n)^2}\Big\langle\log\bar{X}_i-\log M_i,\log\mu-\log M_i\Big\rangle\right|\overset{\text{prob}}{\longrightarrow}0\quad\text{as } p\to\infty. \tag{24}$$

Combining (22), (23), and (24), we have

$$\sup_{\lambda>0,\|\log\mu\|\le\max_{1\le i\le p}\|\log\bar{X}_i\|}\left|\mathrm{SURE}_1(\lambda,\mu)-L_1\big(\widehat{\boldsymbol{M}}^{\lambda,\mu},\boldsymbol{M}\big)\right|\overset{\text{prob}}{\longrightarrow}0\quad\text{as } p\to\infty. \tag{25}$$

For the second term, we have

$$
\begin{aligned}
&|\mathrm{SURE}_2(\Psi,\nu) - L_2\big(\widehat{\mathbf{\Sigma}}^{\Psi,\nu},\mathbf{\Sigma}\big)| \\
&= \bigg| p^{-1}\sum_{i=1}^{p}(\nu+n-q-2)^{-2}\bigg[2(\nu-q-1)\Big(\frac{\mathrm{tr}(\Psi S_i)}{n-1} - \mathrm{tr}(\Psi\Sigma_i)\Big) \\
&\quad + \frac{(n-1)^2-(\nu-q-1)^2}{(n+1)(n-2)(n-1)}(\mathrm{tr}\,S_i)^2 - \frac{(n-1)^2-(\nu-q-1)^2}{(n+1)(n-2)}\,\mathrm{tr}(S_i^2) \\
&\quad + 2(n-1)\,\mathrm{tr}(S_i\Sigma_i) - \big((n-1)^2+(\nu-q-1)^2\big)\,\mathrm{tr}(\Sigma_i^2) \\
&\quad - 2\big\langle \Psi-(\nu-q-1)\Sigma_i, S_i-(n-1)\Sigma_i\big\rangle\bigg]\bigg| \\
&\le \bigg| p^{-1}\sum_{i=1}^{p}\frac{2(\nu-q-1)(n-1)}{(\nu+n-q-2)^2}\langle\Psi, S_i-(n-1)\,\mathrm{tr}\,\Sigma_i\rangle\bigg| && (26) \\
&\quad + \bigg| p^{-1}\sum_{i=1}^{p} C(\nu)\Big[(\mathrm{tr}\,S_i)^2 - (n-1)^2(\mathrm{tr}\,\Sigma_i)^2 - 2(n-1)\,\mathrm{tr}(\Sigma_i^2)\Big]\bigg| && (27) \\
&\quad + \bigg| p^{-1}\sum_{i=1}^{p}(n-1)C(\nu)\Big[\,\mathrm{tr}(S_i^2) - (n-1)(\mathrm{tr}\,\Sigma_i)^2 - n(n-1)\,\mathrm{tr}(\Sigma_i^2)\Big]\bigg| && (28) \\
&\quad + \bigg| p^{-1}\sum_{i=1}^{p}2(n-1)\Big[\,\mathrm{tr}(S_i\Sigma_i) - (n-1)\,\mathrm{tr}(\Sigma_i^2)\Big]\bigg| && (29) \\
&\quad + \bigg| p^{-1}\sum_{i=1}^{p}\frac{2\big\langle\Psi-(\nu-q-1)\Sigma_i, S_i-(n-1)\Sigma_i\big\rangle}{(\nu+n-q-2)^2}\bigg|. && (30)
\end{aligned}
$$

where

$$
C(\nu) = (\nu+n-q-2)^{-2}\frac{(n-1)^2-(\nu-q-1)^2}{(n+1)(n-2)(n-1)}.
$$

Note that $\sup_{\nu>q-1} C(\nu) = [(n+1)(n-2)(n-1)]^{-1}$.

For (26), by Lemma 4, we have

$$
\begin{aligned}
&\sup_{\nu>q+1,\|\Psi\|\le\max_{1\le i\le p}\|S_i\|}\bigg|p^{-1}\sum_{i=1}^{p}\frac{2(\nu-q-1)(n-1)}{(\nu+n-q-2)^2}\big\langle\Psi, S_i-(n-1)\Sigma_i\big\rangle\bigg| \\
&\le \sup_{\nu>q+1}\left(\frac{2(\nu-q-1)(n-1)}{(\nu+n-q-2)^2}p^{-1}\max_{1\le i\le p}\|S_i\|\left\|\sum_{i=1}^{p}S_i-(n-1)\Sigma_i\right\|\right) \\
&= \frac{2(n-1)^2}{(n-2)^2}\left(p^{-1}\max_{1\le i\le p}\|S_i\|\left\|\sum_{i=1}^{p}S_i-(n-1)\Sigma_i\right\|\right)
\end{aligned}
$$

and

$$
\begin{aligned}
&E\left[\frac{1}{p}\max_{1\le i\le p}\|S_i\|\left\|\sum_{i=1}^{p}S_i-(n-1)\Sigma_i\right\|\right]\\
&\le\frac{1}{p}\left[E\Big(\max_{i\le i\le p}\|S_i\|^2\Big)E\left\|\sum_{i=1}^{p}S_i-(n-1)\Sigma_i\right\|^2\right]^{1/2}\\
&=O(p^{-1})\times O(qp^{1/4}\log p+qp^{1/4}\log q)\times O(p^{1/2})\\
&=O(p^{-1/4}\log p)=o(1).
\end{aligned}
$$

Hence, we have

$$
\sup_{\nu>q+1,\|\Psi\|\le\max_{1\le i\le p}\|S_i\|}\left|p^{-1}\sum_{i=1}^{p}\frac{2(\nu-q-1)(n-1)}{(\nu+n-q-2)^2}\big\langle\Psi,S_i-(n-1)\Sigma_i\big\rangle\right|\xrightarrow{\text{prob}}0\quad\text{as } p\to\infty. \tag{31}
$$

For (27), we have

$$
\begin{aligned}
&\sup_{\nu>q+1}\left|p^{-1}\sum_{i=1}^{p}C(\nu)\Big[(\operatorname{tr}S_i)^2-(n-1)^2(\operatorname{tr}\Sigma_i)^2-2(n-1)\operatorname{tr}(\Sigma_i^2)\Big]\right|\\
&=\frac{1}{(n+1)(n-2)(n-1)}\left|p^{-1}\sum_{i=1}^{p}\Big[(\operatorname{tr}S_i)^2-(n-1)^2(\operatorname{tr}\Sigma_i)^2-2(n-1)\operatorname{tr}(\Sigma_i^2)\Big]\right|
\end{aligned}
$$

and

$$
\begin{aligned}
&\operatorname{Var}\left[p^{-1}\sum_{i=1}^{p}\Big[(\operatorname{tr}S_i)^2-(n-1)^2(\operatorname{tr}\Sigma_i)^2-2(n-1)\operatorname{tr}(\Sigma_i^2)\Big]\right]\\
&=p^{-2}\sum_{i=1}^{p}\operatorname{Var}\Big((\operatorname{tr}S_i)^2-(n-1)^2(\operatorname{tr}\Sigma_i)^2-2(n-1)\operatorname{tr}(\Sigma_i^2)\Big)\\
&=p^{-2}\sum_{i=1}^{p}E\Big((\operatorname{tr}S_i)^2-(n-1)^2(\operatorname{tr}\Sigma_i)^2-2(n-1)\operatorname{tr}(\Sigma_i^2)\Big)^2\\
&=p^{-2}\sum_{i=1}^{p}\Big[E(\operatorname{tr}S_i)^4-\Big((n-1)^2(\operatorname{tr}\Sigma_i)^2+2(n-1)\operatorname{tr}(\Sigma_i^2)\Big)^2\Big]\\
&=p^{-2}\sum_{i=1}^{p}\Big[2^4\sum_{\kappa}\Big(\frac{n-1}{2}\Big)_\kappa C_\kappa(\Sigma_i)-(n-1)^4(\operatorname{tr}\Sigma_i)^4\\
&\quad-4(n-1)^3(\operatorname{tr}\Sigma_i)^2\operatorname{tr}(\Sigma_i^2)-4(n-1)^2\big(\operatorname{tr}(\Sigma_i^2)\big)^2\Big]\xrightarrow{p\to\infty}0\quad(\text{by (17)}).
\end{aligned}
$$

By Markov's inequality, we have

$$
\left|p^{-1}\sum_{i=1}^{p}\Big[(\operatorname{tr}S_i)^2-(n-1)^2(\operatorname{tr}\Sigma_i)^2-2(n-1)\operatorname{tr}(\Sigma_i^2)\Big]\right|\xrightarrow{\text{prob}}0\quad\text{as } p\to\infty. \tag{32}
$$

Remark 2 By Lemma 1, assumption (i) implies $\limsup_{p\to\infty} p^{-1}\sum_{i=1}^{p} C_\kappa(\Sigma_i) < \infty$ for all partitions $\kappa = (k_1, \ldots, k_q)$ with $\sum_{j=1}^{q} k_j \le 4$.

For (28), we have

$$\begin{aligned}
&\sup_{\nu>q+1}\left|p^{-1}\sum_{i=1}^{p}(n-1)C(\nu)\Big[\operatorname{tr}(S_i^2)-(n-1)(\operatorname{tr}\Sigma_i)^2-n(n-1)\operatorname{tr}(\Sigma_i^2)\Big]\right| \\
&= \frac{1}{(n+1)(n-2)}\left|p^{-1}\sum_{i=1}^{p}\Big[\operatorname{tr}(S_i^2)-(n-1)(\operatorname{tr}\Sigma_i)^2-n(n-1)\operatorname{tr}(\Sigma_i^2)\Big]\right|
\end{aligned}$$

and

$$\begin{aligned}
&\operatorname{Var}\left[p^{-1}\sum_{i=1}^{p}\Big[\operatorname{tr}(S_i^2)-(n-1)(\operatorname{tr}\Sigma_i)^2-n(n-1)\operatorname{tr}(\Sigma_i^2)\Big]\right] \\
&= p^{-2}\sum_{i=1}^{p}\operatorname{Var}\Big(\operatorname{tr}(S_i^2)-(n-1)(\operatorname{tr}\Sigma_i)^2-n(n-1)\operatorname{tr}(\Sigma_i^2)\Big) \\
&= p^{-2}\sum_{i=1}^{p}E\Big(\operatorname{tr}(S_i^2)-(n-1)(\operatorname{tr}\Sigma_i)^2-n(n-1)\operatorname{tr}(\Sigma_i^2)\Big)^2 \\
&= p^{-2}\sum_{i=1}^{p}\Big[E(\operatorname{tr}(S_i^2))^2-\Big((n-1)(\operatorname{tr}\Sigma_i)^2+n(n-1)\operatorname{tr}(\Sigma_i^2)\Big)^2\Big] \\
&\le p^{-2}\sum_{i=1}^{p}\Big[E(\operatorname{tr}S_i)^4-(n-1)^2(\operatorname{tr}\Sigma_i)^4 \\
&\quad -2n(n-1)^2(\operatorname{tr}\Sigma_i)^2\operatorname{tr}(\Sigma_i^2)-n^2(n-1)^2\big(\operatorname{tr}(\Sigma_i^2)\big)^2\Big] \overset{p\to\infty}{\longrightarrow} 0 \quad \text{(by (17))}.
\end{aligned}$$

By Markov's inequality, we have

$$\left|p^{-1}\sum_{i=1}^{p}\Big[\operatorname{tr}(S_i^2)-(n-1)(\operatorname{tr}\Sigma_i)^2-n(n-1)\operatorname{tr}(\Sigma_i^2)\Big]\right| \overset{\text{prob}}{\longrightarrow} 0 \quad \text{as } p\to\infty. \tag{33}$$

For (29), by Cauchy's inequality, we have

$$\begin{aligned}
\left|p^{-1}\sum_{i=1}^{p}2(n-1)\Big[\operatorname{tr}(S_i\Sigma_i)-(n-1)\operatorname{tr}(\Sigma_i^2)\Big]\right| &= \left|p^{-1}\sum_{i=1}^{p}2(n-1)\langle\Sigma_i, S_i-(n-1)\Sigma_i\rangle\right| \\
&\le 2(n-1)p^{-1}\sum_{i=1}^{p}|\langle\Sigma_i, S_i-(n-1)\Sigma_i\rangle| \\
&\le 2(n-1)p^{-1}\sum_{i=1}^{p}\|\Sigma_i\|\|S_i-(n-1)\Sigma_i\|.
\end{aligned}$$

Then

$$
\begin{aligned}
&\operatorname{Var}\left(2(n-1)p^{-1}\sum_{i=1}^{p}\|\Sigma_i\|\|S_i-(n-1)\Sigma_i\|\right)\\
&=\frac{4(n-1)^2}{p}p^{-1}\sum_{i=1}^{p}\operatorname{Var}\left(\|\Sigma_i\|\|S_i-(n-1)\Sigma_i\|\right)\\
&\le\frac{4(n-1)^2}{p}p^{-1}\sum_{i=1}^{p}E\left(\|\Sigma_i\|^2\|S_i-(n-1)\Sigma_i\|^2\right)\\
&=\frac{4(n-1)^2}{p}p^{-1}\sum_{i=1}^{p}\operatorname{tr}(\Sigma_i^2)\Big[E\operatorname{tr}(S_i^2)-2(n-1)E\operatorname{tr}(S_i\Sigma_i)+(n-1)^2\operatorname{tr}(\Sigma_i^2)\Big]\\
&=\frac{4(n-1)^2}{p}p^{-1}\sum_{i=1}^{p}\operatorname{tr}(\Sigma_i^2)\Big[n(n-1)\operatorname{tr}(\Sigma_i^2)+(n-1)(\operatorname{tr}\Sigma_i)^2-2(n-1)^2\operatorname{tr}(\Sigma_i^2)+(n-1)^2\operatorname{tr}(\Sigma_i^2)\Big]\\
&=\frac{4(n-1)^3}{p}p^{-1}\sum_{i=1}^{p}\left(\operatorname{tr}(\Sigma_i^2)\right)^2+\operatorname{tr}(\Sigma_i^2)(\operatorname{tr}\Sigma_i)^2\overset{p\to\infty}{\longrightarrow}0.
\end{aligned}
$$

By Markov's inequality, we have

$$
\left|p^{-1}\sum_{i=1}^{p}2(n-1)\Big[\operatorname{tr}(S_i\Sigma_i)-(n-1)\operatorname{tr}(\Sigma_i^2)\Big]\right|\overset{\text{prob}}{\longrightarrow}0\quad\text{as } p\to\infty. \tag{34}
$$

For (30), we have

$$
\begin{aligned}
&\sup_{\nu>q+1,\|\Psi\|\le\max_{1\le i\le p}\|S_i\|}\left|p^{-1}\sum_{i=1}^{p}\frac{2\big\langle\Psi-(\nu-q-1)\Sigma_i,S_i-(n-1)\Sigma_i\big\rangle}{(\nu+n-q-2)^2}\right|\\
&\le\sup_{\nu>q+1,\|\Psi\|\le\max_{1\le i\le p}\|S_i\|}\left|p^{-1}\sum_{i=1}^{p}\frac{2\big\langle\Psi,S_i-(n-1)\Sigma_i\big\rangle}{(\nu+n-q-2)^2}\right|\\
&\quad+\sup_{\nu>q+1}\left|p^{-1}\sum_{i=1}^{p}\frac{2(\nu-q-1)\big\langle\Sigma_i,S_i-(n-1)\Sigma_i\big\rangle}{(\nu+n-q-2)^2}\right|\\
&\le\sup_{\|\Psi\|\le\max_{1\le i\le p}\|S_i\|}\left|p^{-1}\sum_{i=1}^{p}2\big\langle\Psi,S_i-(n-1)\Sigma_i\big\rangle\right|+\left|p^{-1}\sum_{i=1}^{p}2\big\langle\Sigma_i,S_i-(n-1)\Sigma_i\big\rangle\right|.
\end{aligned}
$$

Since by assumption (i)

$$
\begin{aligned}
&\operatorname{Var}\left(p^{-1}\sum_{i=1}^{p} 2\langle \Sigma_i, S_i-(n-1)\Sigma_i\rangle\right)\\
&=\frac{1}{p^2}\sum_{i=1}^{p} E\big[\langle \Sigma_i, S_i-(n-1)\Sigma_i\rangle^2\big]\\
&\le \frac{1}{p^2}\sum_{i=1}^{p} E\big[\|\Sigma_i\|^2\|S_i-(n-1)\Sigma_i\|^2\big]\\
&=\frac{1}{p^2}\sum_{i=1}^{p} \|\Sigma_i\|^2 E\big[\operatorname{tr}(S_i^2)-2(n-1)\operatorname{tr}(S_i\Sigma_i)+(n-1)^2\operatorname{tr}(\Sigma_i^2)\big]\\
&=\frac{1}{p^2}\sum_{i=1}^{p} \operatorname{tr}(\Sigma_i^2)\Big[(n-1)\operatorname{tr}(\Sigma_i^2)+(n-1)(\operatorname{tr}\Sigma_i)^2\Big]\\
&\le \frac{n-1}{p^2}\sum_{i=1}^{p}(\operatorname{tr}\Sigma_i)^4 \overset{p\to\infty}{\longrightarrow} 0,
\end{aligned}
$$

by Markov's inequality, we have

$$
\left|p^{-1}\sum_{i=1}^{p} 2\langle \Sigma_i, S_i-(n-1)\Sigma_i\rangle\right| \overset{\text{prob}}{\longrightarrow} 0 \quad \text{as } p\to\infty.
$$

Similarly, we have

$$
\sup_{\|\Psi\|\le \max_{1\le i\le p}\|S_i\|}\left|p^{-1}\sum_{i=1}^{p} 2\langle \Psi, S_i-(n-1)\Sigma_i\rangle\right| \le \frac{2}{p}\max_{1\le i\le p}\|S_i\|\left\|\sum_{i=1}^{p} S_i-(n-1)\Sigma_i\right\|
$$

and

$$
E\left[\frac{2}{p}\max_{1\le i\le p}\|S_i\|\left\|\sum_{i=1}^{p} S_i-(n-1)\Sigma_i\right\|\right]=o(1).
$$

Hence, we have

$$
\sup_{\nu>q+1,\|\Psi\|\le \max_{1\le i\le p}\|S_i\|}\left|p^{-1}\sum_{i=1}^{p}\frac{2\langle \Psi-(\nu-q-1)\Sigma_i, S_i-(n-1)\Sigma_i\rangle}{(\nu+n-q-2)^2}\right| \overset{\text{prob}}{\longrightarrow} 0 \quad \text{as } p\to\infty. \tag{35}
$$

Combining (31), (32), (33), (34), and (35), we have

$$
\sup_{\nu>q+1,\|\Psi\|\le \max_{1\le i\le p}\|S_i\|}\left|\mathrm{SURE}_2(\nu,\Psi)-L_2\big(\widehat{\boldsymbol{\Sigma}}^{\nu,\Psi},\boldsymbol{\Sigma}\big)\right| \overset{\text{prob}}{\longrightarrow} 0 \quad \text{as } p\to\infty. \tag{36}
$$

The proof is concluded by (25) and (36). □

Theorem 4 *If assumptions (i), (ii), and (iii) in Theorem 3 hold, then*

$$\lim_{p\to\infty}\left[R\Big((\widehat{\boldsymbol{M}}^{SURE},\widehat{\boldsymbol{\Sigma}}^{SURE}),(\boldsymbol{M},\boldsymbol{\Sigma})\Big)-R\Big((\widehat{\boldsymbol{M}}^{\lambda,\mu},\widehat{\boldsymbol{\Sigma}}^{\Psi,\nu}),(\boldsymbol{M},\boldsymbol{\Sigma})\Big)\right]\leq 0.$$

Proof. Since

$$\begin{aligned}
&L\Big((\widehat{\boldsymbol{M}}^{\mathrm{SURE}},\widehat{\boldsymbol{\Sigma}}^{\mathrm{SURE}}),(\boldsymbol{M},\boldsymbol{\Sigma})\Big)-L\Big((\widehat{\boldsymbol{M}}^{\lambda,\mu},\widehat{\boldsymbol{\Sigma}}^{\Psi,\nu}),(\boldsymbol{M},\boldsymbol{\Sigma})\Big)\\
&=L\Big((\widehat{\boldsymbol{M}}^{\mathrm{SURE}},\widehat{\boldsymbol{\Sigma}}^{\mathrm{SURE}}),(\boldsymbol{M},\boldsymbol{\Sigma})\Big)-\mathrm{SURE}(\widehat{\lambda}^{\mathrm{SURE}},\widehat{\mu}^{\mathrm{SURE}},\widehat{\Psi}^{\mathrm{SURE}},\widehat{\nu}^{\mathrm{SURE}})\\
&\quad+\mathrm{SURE}(\widehat{\lambda}^{\mathrm{SURE}},\widehat{\mu}^{\mathrm{SURE}},\widehat{\Psi}^{\mathrm{SURE}},\widehat{\nu}^{\mathrm{SURE}})-\mathrm{SURE}(\lambda,\mu,\Psi,\nu)\\
&\quad+\mathrm{SURE}(\lambda,\mu,\Psi,\nu)-L\Big((\widehat{\boldsymbol{M}}^{\lambda,\mu},\widehat{\boldsymbol{\Sigma}}^{\Psi,\nu}),(\boldsymbol{M},\boldsymbol{\Sigma})\Big)\\
&\leq\sup_{\lambda,\mu,\Psi,\nu}\left|L\Big((\widehat{\boldsymbol{M}}^{\lambda,\mu},\widehat{\boldsymbol{\Sigma}}^{\Psi,\nu}),(\boldsymbol{M},\boldsymbol{\Sigma})\Big)-\mathrm{SURE}(\lambda,\mu,\Psi,\nu)\right|\\
&\quad+0\\
&\quad+\sup_{\lambda,\mu,\Psi,\nu}\left|L\Big((\widehat{\boldsymbol{M}}^{\lambda,\mu},\widehat{\boldsymbol{\Sigma}}^{\Psi,\nu}),(\boldsymbol{M},\boldsymbol{\Sigma})\Big)-\mathrm{SURE}(\lambda,\mu,\Psi,\nu)\right|\\
&=2\sup_{\lambda,\mu,\Psi,\nu}\left|L\Big((\widehat{\boldsymbol{M}}^{\lambda,\mu},\widehat{\boldsymbol{\Sigma}}^{\Psi,\nu}),(\boldsymbol{M},\boldsymbol{\Sigma})\Big)-\mathrm{SURE}(\lambda,\mu,\Psi,\nu)\right|,
\end{aligned}$$

from Theorem 3, we have

$$\lim_{p\to\infty}\left[L\Big((\widehat{\boldsymbol{M}}^{\mathrm{SURE}},\widehat{\boldsymbol{\Sigma}}^{\mathrm{SURE}}),(\boldsymbol{M},\boldsymbol{\Sigma})\Big)-L\Big((\widehat{\boldsymbol{M}}^{\lambda,\mu},\widehat{\boldsymbol{\Sigma}}^{\Psi,\nu}),(\boldsymbol{M},\boldsymbol{\Sigma})\Big)\right]\leq 0.$$

Hence, by dominated convergence, we have

$$\begin{aligned}
&\lim_{p\to\infty}\left[R\Big((\widehat{\boldsymbol{M}}^{\mathrm{SURE}},\widehat{\boldsymbol{\Sigma}}^{\mathrm{SURE}}),(\boldsymbol{M},\boldsymbol{\Sigma})\Big)-R\Big((\widehat{\boldsymbol{M}}^{\lambda,\mu},\widehat{\boldsymbol{\Sigma}}^{\Psi,\nu}),(\boldsymbol{M},\boldsymbol{\Sigma})\Big)\right]\\
&=\lim_{p\to\infty}E\left[L\Big((\widehat{\boldsymbol{M}}^{\mathrm{SURE}},\widehat{\boldsymbol{\Sigma}}^{\mathrm{SURE}}),(\boldsymbol{M},\boldsymbol{\Sigma})\Big)-L\Big((\widehat{\boldsymbol{M}}^{\lambda,\mu},\widehat{\boldsymbol{\Sigma}}^{\Psi,\nu}),(\boldsymbol{M},\boldsymbol{\Sigma})\Big)\right]\\
&=E\left\{\lim_{p\to\infty}\left[L\Big((\widehat{\boldsymbol{M}}^{\mathrm{SURE}},\widehat{\boldsymbol{\Sigma}}^{\mathrm{SURE}}),(\boldsymbol{M},\boldsymbol{\Sigma})\Big)-L\Big((\widehat{\boldsymbol{M}}^{\lambda,\mu},\widehat{\boldsymbol{\Sigma}}^{\Psi,\nu}),(\boldsymbol{M},\boldsymbol{\Sigma})\Big)\right]\right\}\\
&\leq 0.
\end{aligned}$$

□

4 Implementation Details

Note that to find the shrinkage estimators $(\widehat{\boldsymbol{M}}^{\lambda,\mu}, \widehat{\boldsymbol{\Sigma}}^{\Psi,\nu})$, we need to solve the optimization problem

$$\min_{\lambda,\mu,\Psi,\nu} \mathrm{SURE}(\lambda, \mu, \Psi, \nu)$$

which is a non-convex optimization problem. Hence the solution depends heavily on the initialization of the minimization algorithm. In this section, we provide a way to choose the initialization so that, in our experiments, the algorithm converges successfully in less than 10 iterations. We can compute the marginal expectations

$$E^{\mathrm{LE}}\big(\bar{X}_i^{\mathrm{LE}}\big) = E_{M_i}^{\mathrm{LE}}\Big[E_X^{\mathrm{LE}}\big(\bar{X}_i^{\mathrm{LE}}|M_i\big)\Big] = E_{M_i}^{\mathrm{LE}}[M_i] = \mu \tag{37}$$

$$\begin{aligned} Ed_{\mathrm{LE}}^2(\bar{X}_i^{\mathrm{LE}}, \mu) &= E_{\Sigma_i}\big\{E_{M_i}\big[E_X\big(d_{\mathrm{LE}}^2(\bar{X}_i^{\mathrm{LE}}, \mu)|M_i, \Sigma_i\big)|\Sigma_i\big]\big\} \\ &= E_{\Sigma_i}\Big[\Big(1/n + 1/\lambda\Big)\operatorname{tr}\Sigma_i\Big] = \left(\frac{1}{n} + \frac{1}{\lambda}\right)\frac{\operatorname{tr}\Psi}{\nu - q - 1} \end{aligned} \tag{38}$$

$$E(S_i) = E_{\Sigma_i}[E_{S_i}(S_i|\Sigma_i)] = E_{\Sigma_i}[(n-1)\Sigma_i] = \frac{n-1}{\nu - q - 1}\Psi \tag{39}$$

$$E(S_i^{-1}) = E_{\Sigma_i}[E_{S_i}(S_i^{-1}|\Sigma_i)] = E_{\Sigma_i}\left[\frac{\Sigma_i^{-1}}{n-q-2}\right] = \frac{\nu}{n-q-2}\Psi^{-1} \tag{40}$$

where $E^{\mathrm{LE}}(\cdot)$ denotes the Fréchet expectation with respect to the Log-Euclidean metric, i.e. $E^{\mathrm{LE}}(X) = \exp(E(\log X))$. Thus the hyperparameters can be written as

$$\begin{aligned} \mu &= E^{\mathrm{LE}}\big(\bar{X}_i^{\mathrm{LE}}\big) \\ \lambda &= \frac{nEd_{\mathrm{LE}}^2(\bar{X}_i^{\mathrm{LE}}, \mu)}{\frac{n}{n-1}E(\operatorname{tr} S_i) - Ed_{\mathrm{LE}}^2(\bar{X}_i^{\mathrm{LE}}, \mu)} \quad \text{(by (38) and (39))} \\ \nu &= \frac{q+1}{\frac{n-q-2}{q(n-1)}\operatorname{tr}(E(S_i)E(S_i^{-1})) - 1} + q + 1 \quad \text{(by (39) and (40))} \\ \Psi &= \frac{\nu - q - 1}{n-1}E(S_i) \quad \text{(by (39))} \end{aligned}$$

and an initialization of the hyperparameters can be obtained by replacing the (Fréchet) expectations with the corresponding sample (Fréchet) means, i.e.

$$\begin{aligned}
\mu_0 &= \exp\left(p^{-1}\sum_{i=1}^{p}\log \bar{X}_i^{\mathrm{LE}}\right)\\
\lambda_0 &= \frac{np^{-1}\sum_{i=1}^{p} d^2_{\mathrm{LE}}(\bar{X}_i^{\mathrm{LE}},\mu_0)}{\frac{n}{p(n-1)}\sum_{i=1}^{p}\operatorname{tr} S_i - p^{-1}\sum_{i=1}^{p} d^2_{\mathrm{LE}}(\bar{X}_i^{\mathrm{LE}},\mu_0)}\\
\nu_0 &= \frac{q+1}{\frac{n-q-2}{p^2q(n-1)}\operatorname{tr}\left[(\sum_{i=1}^{p} S_i)(\sum_{i=1}^{p} S_i^{-1})\right]-1} + q + 1\\
\Psi_0 &= \frac{\nu_0 - q - 1}{p(n-1)}\sum_{i=1}^{p} S_i.
\end{aligned}$$

Note that these initial values can also be viewed as empirical Bayes estimates for μ, λ, ν, and Ψ obtained by matching moments. However these estimates do not possess the asymptotic optimality as stated in Theorem 3 and Theorem 4 since they are not obtained by minimizing an estimate of the risk function.

References

Afsari, B. (2011), 'Riemannian L^p center of mass: Existence, uniqueness, and convexity', *Proceedings of the American Mathematical Society* **139**(02), 655–655.
URL: *http://www.ams.org/jourcgi/jour-getitem?pii=S0002-9939-2010-10541-5*

Alexander, D. C. (2005), 'Multiple-fiber reconstruction algorithms for diffusion MRI', *White Matter in Cognitive Neuroscience: Advances in Diffusion Tensor Imaging and Its Applications* **1064**, 113–133.

Arsigny, V., Fillard, P., Pennec, X. & Ayache, N. (2007), 'Geometric means in a novel vector space structure on symmetric positive-definite matrices', *SIAM Journal on Matrix Analysis and Applications* **29**(1), 328–347.

Basser, P. J., Mattiello, J. & LeBihan, D. (1994), 'MR diffusion tensor spectroscopy and imaging', *Biophysical Journal* **66**(1), 259–267.

Behrens, T. E., Berg, H. J., Jbabdi, S., Rushworth, M. F. & Woolrich, M. W. (2007), 'Probabilistic diffusion tractography with multiple fibre orientations: What can we gain?', *Neuroimage* **34**(1), 144–155.

Bhattacharya, R. & Patrangenaru, V. (2003), 'Large sample theory of intrinsic and extrinsic sample means on manifolds I', *The Annals of Statistics* **31**(1), 1–29.

Bhattacharya, R. & Patrangenaru, V. (2005), 'Large sample theory of intrinsic and extrinsic sample means on manifolds II', *The Annals of Statistics* pp. 1225–1259.

Boothby, W. M. (1986), *An Introduction to Differentiable Manifolds and Riemannian Geometry*, Vol. 120, Academic Press.

Brandwein, A. C. & Strawderman, W. E. (1990), 'Stein estimation: The spherically symmetric case', *Statistical Science* **5**(3), 356–369.

Brandwein, A. C. & Strawderman, W. E. (1991), 'Generalizations of James-Stein estimators under spherical symmetry', *The Annals of Statistics* **19**(3), 1639–1650.

Brown, L. D. (1966), 'On the admissibility of invariant estimators of one or more location parameters', *The Annals of Mathematical Statistics* **37**(5), 1087–1136.

Brown, L. D. & Zhao, L. H. (2012), 'A geometrical explanation of Stein shrinkage', *Statistical Science* **27**(1), 24–30.

Callaghan, P. T. (1993), *Principles of Nuclear Magnetic Resonance Microscopy*, Oxford University Press.

Chakraborty, R. & Vemuri, B. C. (2015), Recursive Fréchet mean computation on the Grassmannian and its applications to computer vision, *in* 'Proceedings of the IEEE International Conference on Computer Vision', pp. 4229–4237.

Chakraborty, R. & Vemuri, B. C. (2019), 'Statistics on the Stiefel manifold: Theory and applications', *The Annals of Statistics* **47**(1), 415–438.

Chefd'Hotel, C., Tschumperlé, D., Deriche, R. & Faugeras, O. (2004), 'Regularizing flows for constrained matrix-valued images', *Journal of Mathematical Imaging and Vision* **20**(1-2), 147–162.

Clevenson, M. L. & Zidek, J. V. (1975), 'Simultaneous estimation of the means of independent Poisson laws', *Journal of the American Statistical Association* **70**(351a), 698–705.

Daniels, M. J. & Kass, R. E. (2001), 'Shrinkage estimators for covariance matrices', *Biometrics* **57**(4), 1173–1184.

Dawid, A. P. (1994), 'Selection paradoxes of Bayesian inference', *Multivariate Analysis and Its Applications (Hong Kong, 1992). IMS Lecture Notes Monograph Series.* **24**, 211–220.

Donoho, D. L., Gavish, M. & Johnstone, I. M. (2018), 'Optimal shrinkage of eigenvalues in the spiked covariance model', *The Annals of Statistics* **46**(4), 1742–1778.

Dryden, I. L., Koloydenko, A. & Zhou, D. (2009), 'Non-Euclidean statistics for covariance matrices, with applications to diffusion tensor imaging', *The Annals of Applied Statistics* **3**(3), 1102–1123.

Du, L. & Hu, I. (2019), 'An empirical Bayes method for chi-squared data', *arXiv:1903.00776* .

Efron, B. (2011), 'Tweedies formula and selection bias', *Journal of the American Statistical Association* **106**(496), 1602–1614.

Efron, B. & Morris, C. (1971), 'Limiting the risk of Bayes and empirical Bayes estimators, part I: The Bayes case', *Journal of the American Statistical Association* **66**(336), 807–815.

Efron, B. & Morris, C. (1972*a*), 'Empirical Bayes on vector observations: An extension of Stein's method', *Biometrika* **59**(2), 335–347.

Efron, B. & Morris, C. (1972*b*), 'Limiting the risk of Bayes and empirical Bayes estimators, part II: The empirical Bayes case', *Journal of the American Statistical Association* **67**(337), 130–139.

Efron, B. & Morris, C. (1973*a*), 'Combining possibly related estimation problems', *Journal of the Royal Statistical Society: Series B* **35**(3), 379–402.

Efron, B. & Morris, C. (1973*b*), 'Stein's estimation rule and its competitors: An empirical Bayes approach', *Journal of the American Statistical Association* **68**(341), 117–130.

Efron, B. & Tibshirani, R. (1996), 'Using specially designed exponential families for density estimation', *The Annals of Statistics* **24**(6), 2431–2461.

Fienberg, S. E. & Holland, P. W. (1973), 'Simultaneous estimation of multinomial cell probabilities', *Journal of the American Statistical Association* **68**(343), 683–691.

Fletcher, P. T. & Joshi, S. (2004), Principal geodesic analysis on symmetric spaces: Statistics of diffusion tensors, *in* 'Computer Vision and Mathematical Methods in Medical and Biomedical Image Analysis', Springer, pp. 87–98.

Fletcher, P. T., Joshi, S., Lu, C. & Pizer, S. M. (2003), Gaussian distributions on Lie groups and their application to statistical shape analysis, *in* 'Biennial International Conference on Information Processing in Medical Imaging', Springer, pp. 450–462.

Fréchet, M. (1948), 'Les éléments aléatoires de nature quelconque dans un espace distancié', *Annales de l'Institut Henri Poincaré* **10**(4), 215–310.

Groisser, D. (2004), 'Newton's method, zeroes of vector fields, and the Riemannian center of mass', *Advances in Applied Mathematics* **33**(1), 95–135.

Gupta, A. K. & Nagar, D. K. (2000), *Matrix Variate Distributions*, Chapman and Hall/CRC.

Haff, L. R. (1991), 'The variational form of certain Bayes estimators', *The Annals of Statistics* **19**(3), 1163–1190.

Helgason, S. (2001), *Differential geometry, Lie groups and symmetric spaces*, American Mathematical Society.

Ho, J., Cheng, G., Salehian, H. & Vemuri, B. (2013), Recursive Karcher expectation estimators and geometric law of large numbers, *in* 'Artificial Intelligence and Statistics', PMLR, pp. 325–332.

James, W. & Stein, C. (1962), Estimation with quadratic loss, *in* 'Proceedings of the Fourth Berkeley Symposium on Mathematical Statistics and Probability', Vol. 1, University of California Press, pp. 361–379.

Jing, B.-Y., Li, Z., Pan, G. & Zhou, W. (2016), 'On SURE-type double shrinkage estimation', *Journal of the American Statistical Association* **111**(516), 1696–1704.

Johnson, B. M. (1971), 'On the admissible estimators for certain fixed sample binomial problems', *The Annals of Mathematical Statistics* **42**(5), 1579–1587.

Johnson, R. A. & Wichern, D. W. (2007), *Applied Multivariate Statistical Analysis*, 6th edn, Prentice Hall, Upper Saddle River, NJ.

Kong, X., Liu, Z., Zhao, P. & Zhou, W. (2017), 'SURE estimates under dependence and heteroscedasticity', *Journal of Multivariate Analysis* **161**, 1–11.

Kubokawa, T., Robert, C. P. & Saleh, A. K. M. E. (1993), 'Estimation of noncentrality parameters', *The Canadian Journal of Statistics/La Revue Canadienne de Statistique* **21**(1), 45–57.

Ledoit, O. & Wolf, M. (2003), 'Improved estimation of the covariance matrix of stock returns with an application to portfolio selection', *Journal of Empirical Finance* **10**(5), 603–621.

Ledoit, O. & Wolf, M. (2012), 'Nonlinear shrinkage estimation of large-dimensional covariance matrices', *The Annals of Statistics* **40**(2), 1024–1060.

Lenglet, C., Rousson, M. & Deriche, R. (2006), 'DTI segmentation by statistical surface evolution', *IEEE Transactions on Medical Imaging* **25**(6), 685–700.

Lim, Y. & Pálfia, M. (2014), 'Weighted inductive means', *Linear Algebra and its Applications* **453**, 59–83.

Moakher, M. (2005), 'A differential geometric approach to the geometric mean of symmetric positive-definite matrices', *SIAM Journal on Matrix Analysis and Applications* **26**(3), 735–747.

Muirhead, R. J. (1982), *Aspects of Multivariate Statistical Theory*, John Wiley & Sons.

Prodoehl, J., Li, H., Planetta, P. J., Goetz, C. G., Shannon, K. M., Tangonan, R., Comella, C. L., Simuni, T., Zhou, X. J., Leurgans, S., Corcos, D. M. & Vaillancourt, D. E. (2013), 'Diffusion tensor imaging of Parkinson's disease, atypical Parkinsonism, and essential tremor', *Movement Disorders* **28**(13), 1816–1822.

Robbins, H. (1956), An empirical Bayes approach to statistics, *in* 'Proceedings of the Third Berkeley Symposium on Mathematical Statistics and Probability, Volume 1: Contributions to the Theory of Statistics', University of California Press, Berkeley, Calif., pp. 157–163. **URL:** *https://projecteuclid.org/euclid.bsmsp/1200501653*

Salehian, H., Chakraborty, R., Ofori, E., Vaillancourt, D. & Vemuri, B. C. (2015), 'An efficient recursive estimator of the Fréchet mean on a hypersphere with applications to medical image analysis', *Mathematical Foundations of Computational Anatomy* **3**, 143–154.

Sasaki, H., Noh, Y.-K., Niu, G. & Sugiyama, M. (2016), 'Direct density derivative estimation', *Neural Computation* **28**(6), 1101–1140.

Schwartzman, A. (2006), Random Ellipsoids and False Discovery Rates: Statistics for Diffusion Tensor Imaging Data, PhD thesis, Stanford University.

Schwartzman, A. (2016), 'Lognormal distributions and geometric averages of symmetric positive definite matrices', *International Statistical Review* **84**(3), 456–486.

Schwartzman, A., Dougherty, R. F. & Taylor, J. E. (2008), 'False discovery rate analysis of brain diffusion direction maps', *The Annals of Applied Statistics* **2**(1), 153–175.

Shen, W. & Ghosal, S. (2017), 'Posterior contraction rates of density derivative estimation', *Sankhya A* **79**(2), 336–354.

Silverman, B. W. (1986), *Density Estimation for Statistics and Data Analysis*, Chapman and Hall.

Stein, C. (1956), Inadmissibility of the usual estimator for the mean of a multivariate normal distribution, *in* 'Proceedings of the Third Berkeley Symposium on Mathematical Statistics and Probability, 1954–1955, vol. I', University of California Press, Berkeley and Los Angeles, pp. 197–206.

Stein, C. (1959), 'The admissibility of Pitman's estimator of a single location parameter', *The Annals of Mathematical Statistics* **30**(4), 970–979.

Stein, C. (1975), Estimation of a covariance matrix, *in* 'Reitz Lecture, 39th Annual Meeting IMS. Atlanta, Georgia'.

Stein, C. (1981), 'Estimation of the mean of a multivariate normal distribution', *The Annals of Statistics* **9**(6), 1135–1151.

Sturm, K.-T. (2003), 'Probability measures on metric spaces of nonpositive curvature', *Heat Kernels and Analysis on Manifolds, Graphs, and Metric Spaces: Lecture Notes from a Quarter Program on Heat Kernels, Random Walks, and Analysis on Manifolds and Graphs: April 16-July 13, 2002, Emile Borel Centre of the Henri Poincaré Institute, Paris, France* **338**, 357–390.

Terras, A. (2012), *Harmonic Analysis on Aymmetric Apaces and Applications II*, Springer Science & Business Media.

Tsui, K.-W. (1981), 'Simultaneous estimation of several Poisson parameters under squared error loss', *Annals of the Institute of Statistical Mathematics* **33**(1), 215–223.

Tsui, K.-W. & Press, S. J. (1982), 'Simultaneous estimation of several Poisson parameters under k-normalized squared error loss', *The Annals of Statistics* **10**(1), 93–100.

Vaillancourt, D., Spraker, M., Prodoehl, J., Abraham, I., Corcos, D., Zhou, X., Comella, C. & Little, D. (2009), 'High-resolution diffusion tensor imaging in the substantia nigra of de novo Parkinson disease', *Neurology* **72**(16), 1378–1384.

Wang, Z. & Vemuri, B. C. (2004), Tensor field segmentation using region based active contour model, *in* 'European Conference on Computer Vision', Springer, pp. 304–315.

Xie, X., Kou, S. & Brown, L. D. (2012), 'SURE estimates for a heteroscedastic hierarchical model', *Journal of the American Statistical Association* **107**(500), 1465–1479.

Xie, X., Kou, S. C. & Brown, L. (2016), 'Optimal shrinkage estimation of mean parameters in family of distributions with quadratic variance', *The Annals of Statistics* **44**(2), 564–597.

Yang, C.-H. & Vemuri, B. C. (2019), Shrinkage estimation on the manifold of symmetric positive-definite matrices with applications to neuroimaging, *in* 'International Conference on Information Processing in Medical Imaging', Springer, pp. 566–578.

Zhou, D., Dryden, I. L., Koloydenko, A. & Li, B. (2008), A Bayesian method with reparameterization for diffusion tensor imaging, *in* 'Medical Imaging 2008: Image Processing', Vol. 6914, International Society for Optics and Photonics, p. 69142J.